

AN ABSTRACT OF THE THESIS OF

Craig L. Moyer for the degree of Master of Science in

Microbiology presented on April 22, 1988

Title: GROWTH RATE EFFECTS DURING STARVATION-SURVIVAL OF
A MARINE PSYCHROPHILIC VIBRIO

Redacted for Privacy

Abstract Approved:

~~Dr. Richard Y. Morita~~

Cell populations of the marine bacterium ANT-300, from either batch culture or continuous culture with dilution rates ranging from $D = 0.170 \text{ h}^{-1}$ (fast) to $D = 0.015 \text{ h}^{-1}$ (slow) were monitored for 98 days under starvation. Viability (CFU), acridine orange direct counts (AODC), and optical density were measured. DNA, RNA, and protein concentrations were also estimated on a total and viable cell basis. A new method for the assay of nucleic acids was developed for this study.

Three viability patterns of starvation-survival were observed for each of the cell populations. AODC cells remained at $2-3 \times 10^7$ cells per ml throughout the starvation period. Large fluctuations occurred in cell viability during stage 1 (0 to 14 days) of starvation-survival. Stage 2 (14 to 70 days) involved an overall decrease in viability for each of the cell populations,

with the rate of viability loss being dependent upon the growth rate. Cell viability stabilized at approximately 0.3% of the AODC cell number in stage 3 (70 to 98 days). Long-term starvation was the prolongation of stage 3 starvation-survival. Biovolumes for each of the cell populations decreased with the length of the starvation period. However, the biovolume of starved cells depended on growth rate more than the length of time starved.

DNA, RNA, and protein concentrations on a total and viable cell basis fluctuated corresponding to the three stages of starvation-survival. During stage 1 of starvation-survival, 2-3 peaks in the concentration levels for all three macromolecules were characteristic. DNA per total cell in stage 2 dropped to 4.2 - 8.3% for all of the cell populations examined, and then stabilized throughout stage 3. The decrease in DNA per cell was also observed in electron micrographs of cellular DNA in starved and unstarved ANT-300 cells. The fluctuations of RNA and protein concentrations observed during stage 2 and 3 were parallel in all cases except for the cells from $D = 0.015 \text{ h}^{-1}$. This ANT-300 cell population showed a decrease in RNA to 29.2% and an increase in protein to 129.7% of original concentrations. RNA and protein concentrations also stabilized in stage 3. The cells from the faster growth rate cell populations of $D = 0.170 \text{ h}^{-1}$ and batch culture had elevated protein concentrations, which remained mostly residual during the starvation

period. Macromolecule ratio data indicate two phenomena:

(i) The $D = 0.015 \text{ h}^{-1}$ cells demonstrate the production and maintenance of protein relative to diminished RNA levels.

(ii) The $D = 0.057 \text{ h}^{-1}$ cells suggest the existence of a transitory state between the high efficiency of the $D = 0.015 \text{ h}^{-1}$ cells and the high residuals of the $D = 0.170 \text{ h}^{-1}$ and batch culture cells.

It has been demonstrated that three stages of starvation-survival exist as indicated by cell counts and the estimation of DNA, RNA, and protein, for all the cell populations examined. Slow growth rate ($D = 0.015 \text{ h}^{-1}$) cells indicate enhanced viability during the starvation period, and the capability to produce and maintain relatively high protein levels per cell. These cells exhibit low concentrations of RNA per cell, thus yielding more efficient translation and maintenance capabilities under starvation conditions. Cells from this population also have the lowest biovolume, corresponding to the greatest surface area during the starvation period. Therefore, it is hypothesized that under starvation-survival conditions the ANT-300 population of slow growth rate cells ($D = 0.015 \text{ h}^{-1}$) are the closest representatives to cells found in the marine environment at in situ growth rates.

GROWTH RATE EFFECTS DURING STARVATION-SURVIVAL OF
A MARINE PSYCHROPHILIC VIBRIO

by

Craig Lee Moyer

A THESIS

submitted to

Oregon State University

in partial fulfillment of
the requirements for the
degree of

Master of Science

Completed April 22, 1988

Commencement June 1988

APPROVED:

Redacted for Privacy

Professor of Microbiology in charge of major

Redacted for Privacy

Chairman of Microbiology Department

Redacted for Privacy

Dean of Graduate School

Date thesis is presented

April 22, 1988

ACKNOWLEDGEMENTS

I gratefully acknowledge my mentor, Dr. R.Y. Morita for his knowledge, skills, and wisdom; and for his willingness to share those qualities with me. I am also deeply grateful to the varsity team (Dr. R.P. Griffiths and Bruce Caldwell) for their stimulation, help, and advice. I would like to acknowledge and thank Dr. David Carlson for the use of his laboratory and for the impetus behind constructing the new assay, and Dr. Ian Dundas for the theoretical background of chemostat preparation. A special thanks to my family (Hi Mom) and friends for all the support and encouragement I have received from them. This work was supported by the Bowerman Foundation Scholarship, Tartar Research Fellowship, and EPA Cooperative Agreement CR-913413-01-0.

TABLE OF CONTENTS

	Page
INTRODUCTION	1
MATERIALS AND METHODS	5
Organism and media	5
Growth and starvation conditions	7
Viability determination	9
Direct counts	9
Biovolume determination	10
Nucleic acid assay	11
Protein assay	12
DNA electron microscopy	13
RESULTS AND DISCUSSION	14
Viability assessment	14
Biovolume assessment	30
Macromolecule fluctuations	37
DNA electron micrographs	61
Macromolecule ratios	61
Summary	79
LITERATURE CITED	81

LIST OF FIGURES

Figure	Page
1. Total cells, viable cells, and optical density with starvation time for cells from $D = 0.015 \text{ h}^{-1}$.	17
2. Total cells, viable cells, and optical density with starvation time for cells from $D = 0.057 \text{ h}^{-1}$.	19
3. Total cells, viable cells, and optical density with starvation time for cells from $D = 0.170 \text{ h}^{-1}$.	21
4. Total cells, viable cells, and optical density with starvation time for cells from batch culture.	23
5. Total cells, viable cells, and optical density with starvation time for cells from $D = 0.200 \text{ h}^{-1}$. Long-term study.	26
6. Biovolume of unstarved cells.	33
7. Biovolume of starved cells.	35
8. DNA, RNA, and protein per total cell with starvation time for cells from $D = 0.015 \text{ h}^{-1}$.	38
9. DNA, RNA, and protein per total cell with starvation time for cells from $D = 0.057 \text{ h}^{-1}$.	40
10. DNA, RNA, and protein per total cell with starvation time for cells from $D = 0.170 \text{ h}^{-1}$.	42
11. DNA, RNA, and protein per total cell with starvation time for cells from batch culture.	44
12. DNA, RNA, and protein per viable cell with starvation time for cells from $D = 0.015 \text{ h}^{-1}$.	52
13. DNA, RNA, and protein per viable cell with starvation time for cells from $D = 0.057 \text{ h}^{-1}$.	54

14.	DNA, RNA, and protein per viable cell with starvation time for cells from $D = 0.170 \text{ h}^{-1}$.	56
15.	DNA, RNA, and protein per viable cell with starvation time for cells from batch culture.	58
16.	Electron micrographs of the DNA molecule from logarithmic growth unstarved and starved cells.	62
17.	DNA/RNA ratios with starvation time.	64
18.	DNA/protein ratios with starvation time.	66
19.	RNA/DNA ratios with starvation time.	68
20.	RNA/protein ratios with starvation time.	70
21.	Protein/DNA ratios with starvation time.	72
22.	Protein/RNA ratios with starvation time.	74

LIST OF TABLES

Table	Page
1. ANT-300 dilution rates, with corresponding growth rates, and doubling times.	15
2. Biovolume measurements for starved and unstarved ANT-300 cells.	31

GROWTH RATE EFFECTS DURING STARVATION-SURVIVAL OF A MARINE PSYCHROPHILIC VIBRIO

INTRODUCTION

The survival of heterotrophic marine bacteria is dependent upon the ability to withstand long periods of nutrient deprivation. Below the photic zone, the ocean becomes extremely deficient in nutrients, resulting in a low average level of organic carbon present in the open ocean. The dissolved organic carbon (DOC) concentration ranges from 0.35 to 70 mg per liter and the particulate organic carbon (POC) concentration ranges from 3 to 10 mg per liter (Menzel and Ryther, 1970). Generally, the POC concentration is equal to 10% of the DOC concentration in the open ocean. Both DOC and POC have been found to be refractory to bacterial degradation. Barber (1968) observed no significant change in the levels of deep ocean DOC incubated over two months with viable marine bacteria. However, it has been demonstrated that deep ocean POC hydrolyzed either enzymatically (Gordon, 1970), or chemically (Seki et al., 1968) can then be used for growth by certain marine bacteria. Tranvik and Höfle (1987) found the fraction of DOC consumed by heterotrophic bacteria to range from 15 to 22% of the total DOC pool from various clear and humic fresh water sources. Geller (1986)

observed 12 to 22% decomposition of lake dissolved organic matter (DOM) original macromolecules attributed to bacterial degradation. It is therefore unclear how much DOC and POC is bioavailable. Craig (1971) calculates the total deep-ocean oxygen consumption to be 0.004 ml per liter per yr, indicating a low metabolic activity for all organisms. Morita (1980), in his review of microbial life in the deep ocean suggests that the low concentrations of nutrients becomes a factor that must be reconciled with residence time for deep ocean waters. This residence time can be on the order of 1000 years (Broecker, 1963). The turnover time for DOM has been estimated by Menzel (1974) to be 3,300 years. More recently, Williams and Druffel (1987) have estimated DOC residence times of about 6000 years. These factors suggest that the deep ocean is indeed low in utilizable nutrients and that starvation conditions do exist.

The marine environment is a complex and dynamic ecosystem that is difficult to simulate under laboratory conditions. To control the types of variation which occur naturally, and still attempt to approach in situ growth rates, continuous culture technology may be utilized. Bacteria can be grown under well-defined, reproducible conditions where all environmental parameters are kept constant, resulting in a steady-state population with a uniform growth rate. These populations can be used to

study the effects of starvation-survival on the physiology of cells grown at various rates. The cell populations can be compared entirely on the basis of the growth rate from which the respective population originated prior to starvation. Growth rates of natural assemblages of thymidine-incorporating, marine bacteria have been estimated at 0.036 to 0.075 h⁻¹ (Douglas et al., 1987). Specific growth rates as low as 0.005 h⁻¹ have been estimated by Jannasch (1969) and by Carlucci and Williams (1978) for pelagic marine bacteria. However, it should be remembered that when chemostats are utilized, the system will undergo washout when in situ values of organic matter are used, making continuous culture impossible (Jannasch, 1967 and 1970).

ANT-300, a marine psychrophilic Vibrio, was isolated in 1972 from the waters of the Antarctic Convergence by P.A. Gillespie and L.P. Jones (cf. Baross et al., 1974). ANT-300 has since been intensely examined and has become a model marine heterotrophic bacterium for starvation-survival studies (Morita, 1982). ANT-300 has demonstrated the ability to survive for longer than a year without the addition of an organic energy source (Novitsky and Morita, 1976; 1977; 1978). It was also found to exhibit and maintain an endogenous metabolism of 0.0071% total carbon respired per h after one week and remained constant thereafter for three more weeks (Novitsky and Morita,

1977). ANT-300 has been found to survive under these conditions for up to 2.5 years retaining viability, until the experiment was terminated by a power outage (Morita, 1985). Specific physiological parameters such as the concentration of the macromolecules DNA, RNA, and protein have also been measured during the starvation-survival of ANT-300 by Amy et al. (1983). However, these studies all used cell populations which were originally grown under nutrient rich conditions.

This study examined the physiological changes during starvation-survival, due entirely to the growth rate effects of ANT-300 cells in minimal salts solution devoid of any additional organic carbon or nitrogen. This was done to simulate the extended nutrient deprivation conditions found in the open ocean environment. The objective of this study was to determine if slow growth cells are better adapted to starvation-survival than cells grown under the usual nutrient rich laboratory conditions.

MATERIALS AND METHODS

Organism and Media

ANT-300, a heterotrophic, psychrophilic marine bacterium has been tentatively identified as a Vibrio sp. (Baross et al., 1974). ANT-300 was isolated in 1972 from the Antarctic Convergence at station #18 during cruise #46 of the R/V Eltanin from a depth of 300 m.

Continuous culture cells used in this study were grown using 1/10th strength Lib-X (SLX) medium pumped into chemostats, each containing a total volume of 345 ml. Full strength Lib-X medium was used for cells grown in batch culture. The formulas for the various media are as follows:

1/10th STRENGTH LIB-X (SLX)

Trypticase-peptone (BBL)	0.23 g
Yeast Extract (Difco)	0.12 g
L-glutamic acid	0.03 g
Sodium citrate	0.03 g
NaNO ₃	0.05 g
Fe/EDTA	0.007 g
Rila Salts	38.0 g
Tris Buffer	3.2 g
Distilled water	1.0 liter
pH	7.8

FULL STRENGTH LIB-X

Trypticase-peptone (BBL)	2.3	g
Yeast Extract (Difco)	1.2	g
L-glutamic acid	0.3	g
Sodium citrate	0.3	g
NaNO ₃	0.05	g
Fe/EDTA	0.007	g
Rila Salts	38.0	g
Tris Buffer	3.2	g
Distilled water	1.0	liter
pH	7.8	

BUFFERED 4% SALT MIXTURE (SM)

NaCl	26.0	g
KCl	0.8	g
MgCl ₂ ·6H ₂ O	5.6	g
MgSO ₄ ·7H ₂ O	7.6	g
Tris Buffer	3.2	g
Distilled water	1.0	liter
pH	7.8	

The pH was adjusted using 10 N HCl or 10 N NaOH. The Lib-X media used was modified from the original formula (Baross et al., 1974) in order to adapt it to chemostat systems. Fe/EDTA was utilized due to its increased solubility within the chemostat apparatus. Tris buffer [tris(hydroxy-amino)methane] was included to maintain the pH of the growth media at 7.8 within the chemostat. Lib-X and SLX media were sterilized by use of an autoclave (121°C, 2 atm, 15 min). SM and all reagents used were heat and filter sterilized (twice through 0.45 µm Millipore filters), in order to minimize debris interference with macromolecular assays and total cell counts.

Growth and Starvation Conditions

Due to the psychrophilic nature of ANT-300, all materials were held at 5°C prior to use, including pipette tips, centrifuge bottles, and starvation menstrooms. All glassware was precleaned by autoclaving with RBS-35 (Pierce) washing solution and rinsing thoroughly with double distilled water before sterilization to protect against contamination. ANT-300 cell populations were monitored during growth and starvation spectrophotometrically using a Bausch and Lomb Spectronic 710 spectrophotometer at 600 nm.

Chemostats were constructed so that the growth media (SLX), incoming and outgoing, only came in contact with

silicone or borosilicate glass. The dilution rate in each chemostat was set and maintained constant using a Crouzet mini-peristaltic pump. Chemostats were also supplied with a constant supply of air, which was cotton filter sterilized. The air flow was used to maintain aerobic conditions, and to achieve uniform mixing within the chemostat. ANT-300 cells, that had been cultivated at 5°C in SLX, were used to inoculate each chemostat. SLX medium was used as the dilution medium for all growth experiments. The populations in each chemostat were brought to equilibrium (10-12 generations at each dilution rate) and then harvested. Batch cells were cultivated in Lib-X at 5°C in a 2.8 liter Fernbach flask and shaken at 100 rpm on a rotary shaker (New Brunswick Rotary Model G2) until an OD₆₀₀ of 0.8 was attained (log growth phase). ANT-300 cells were harvested by centrifugation (4080 x g, 15 min at 3°C, Sorvall RC2-B) from the various growth conditions and were washed twice in cold SM. The washed cells were then resuspended in 4 liters of cold SM in sterile 4 liter aspirator bottles, containing a teflon stirring bar, to an initial cell density of ca. $1.5 - 3.5 \times 10^7$ per ml for the duration of 98 days, except for the long-term study which lasted 175 days. Prior to taking samples, each cell suspension was stirred on a magnetic stirrer for 5 min in order to ensure uniform suspension.

ANT-300 cell samples were routinely taken from

starvation menstruums containing the various cell populations and processed immediately. Subsamples were frozen and maintained at -70°C until assayed for macromolecules.

Viability Determination

Colony forming units (CFU) were determined by the spread plate technique. After appropriate dilutions were made, 0.1 ml was spread onto plates containing SLX medium plus 1.2% agar, and incubated for 7 to 10 days, after which cells were considered viable if they produced a visible colony. Quadruplicate determinations were made and averaged in all cases. SLX medium was chosen for plate counts due to the high recovery rate for ANT-300 after starvation as shown by Novitsky (1977, Ph.D. thesis, Oregon State University).

Direct Counts

Direct counts were obtained by acridine orange staining and epifluorescent microscopy (AODC). This method was essentially developed by Francisco et al. (1973), and modified by the use of Nuclepore filters as described by Zimmermann and Meyer-Reil (1974). The procedure was further modified by the use of Irgalan black darkened filters (Hobbie et al., 1977; Watson et al., 1977). Since that time it has been improved by Hoff (1984, Ph.D. thesis,

University of Bergen, Norway) for marine bacteria that exhibited cellular lysis upon using earlier procedures. Samples were fixed with buffered formalin (final concentration of 1%), and then filtered on to Nuclepore filters (0.2 μm pore size). Silver membrane prefilters (Selas Flotronics, 0.8 μm pore size) were used as supports for the Nuclepore filters to ensure uniform cell distribution. After staining, filters were air dried, and then mounted in oil on glass slides with cover slips on top. Preparations were viewed with a Zeiss epifluorescent microscope. Ten to twenty fields were counted for each sample and averaged. The total number of cells per ml was calculated using corresponding dilution factors and a microscopic factor (area conversion and magnification).

Biovolume Determination

ANT-300 cell volumes were determined by sizing acridine orange stained cells from the various cell populations. Because of the significant cell shrinkage (up to 37%) which occurs in the preparation of cells for the electron microcopy, epifluorescence microscopy was used to determine cell sizes (Fuhrman, 1981). Cells were stained using the same procedure as for AODC, above. Measurements were made from projected images of cells and substage micrometer. Cell sizes were calculated against a substage micrometer, averaging 20 cells from each population. The

formulas $V = 4/3\pi r^3$ and $V = \pi r^2 h$ were used to calculate the volumes of starved (spherical) and unstarved (cylindrical) cells, respectively.

Nucleic Acid Assay

Nucleic acids were estimated fluorimetrically using the bifunctional intercalating compound, ethidium homodimer (Molecular Probes, Eugene, Ore.). Bifunctional intercalators such as ethidium homodimer have been demonstrated to have exceptionally high binding affinities for nucleic acids (Le Pecq et al., 1975; Gaugain et al., 1978a, 1978b). Ethidium homodimer has also been shown to be significantly more sensitive than ethidium bromide with sensitivities in the ng/ml range (Markovits et al., 1979) binding to both RNA and DNA.

Cell samples plus 0.1% (vol/vol) 10% Triton-X 100 were treated with sonication (Sonifer Model 350, Branson) for 30 s. Half of the samples were treated with 0.1% (vol/vol) of 10 mg/ml RNase A (Sigma Chem. Co.) and were incubated in a water bath at 37°C for 30 min. These samples were used to measure DNA concentrations. The other half of the samples were used to measure both DNA and RNA concentrations. All subsamples had 32.6 μ M of ethidium homodimer added (final volume). The subsamples were measured with a spectrofluorometer (Perkin-Elmer; model MPF-66) operating in ratio mode (excitation, 300 nm;

emission, 620 nm; emission filter, 610 nm; slit width, 20 nm for both monochromators).

Standard curves were prepared for both DNA and RNA (Sigma Chem. Co.). Controls were made with DNA plus RNase A and with RNA plus RNase A added. These were measured over the same range as the standard curves. Blank controls were also measured to insure precision. DNA concentrations were estimated from fluorescence of the RNase A treated samples measured against the DNA standard curve. RNA concentrations were then estimated by subtracting the fluorescence for RNase A treated samples from the corresponding fluorescence of the untreated sample and measuring this value against the RNA standard curve. Subsample readings were taken in duplicate.

Protein Assay

Total protein was measured by a new highly sensitive method using bicinchoninic acid (BCA) (Smith et al., 1985). Protein concentrations in the range of 0.5 to 10.0 µg/ml were measured using the Micro Reagent procedure also described by Smith et al. (1985).

Prior to running the standard Micro Reagent procedure, cell samples with 0.1% (vol/vol) of 10% Triton-X 100 were treated with sonication for 30 s. The only alterations made from the standard Micro Reagent procedure (Smith et al., 1985) were: 0.16% (wt/vol) was used in the preparation

of Micro reagent A instead of 1.6% (wt/vol), and the sample size volume in the reaction tube was doubled in order to achieve better reproducibility.

Protein concentrations were estimated against a standard curve prepared for each sampling set. All samples were measured in quadruplicate to enhance accuracy, using a Bausch and Lomb Spectronic 710 spectrophotometer at 562 nm.

DNA Electron Microscopy

The DNA from ANT-300 cells was extracted and isolated for electron microscopy analysis using a modified alkaline lysis (Maniatis, 1982). This was done to isolate total DNA from the cells and keep it intact, while eliminating as much cellular debris as possible. The DNA was then resuspended to approximately 5 $\mu\text{g/ml}$ ($\text{OD}_{260} \approx 0.1$) in a 50 mM NaCl and 5 mM EDTA solution ($\text{pH} = 7.5$). The DNA was made hydrophobic, and then transferred onto Formvar copper coated grids. DNA samples were chromium shadowed under a vacuum and viewed with a Philips EM 300 microscope.

RESULTS AND DISCUSSION

Dilution rates with corresponding growth rates and doubling times (t_d) for each of the cell suspensions used during this study are listed in Table 1. These cells originated from growth in continuous culture or batch culture with known growth rates and doubling times. ANT-300 cell populations with doubling times ranging from 3.5 h to 46.2 h (Table 1) were monitored to examine the physiological shifts which occurred on the population and cellular level.

Viability Assessment

Total and viable cell counts as well as turbidity of ANT-300 cell suspensions undergoing starvation are shown in Figs. 1-5. At the beginning of the starvation period the concentrations of viable cells and total cells were approximately the same in all cell populations. The viability of cells from $D = 0.015 \text{ h}^{-1}$ (Fig. 1) began to significantly decrease after approximately 56 days of starvation where it then dropped nearly two orders of magnitude within 1 week. After 70 days of starvation, viability stabilized at approximately 10^5 viable cells per ml. This corresponds to 0.3% viability of the total cell number which remained at approximately 3×10^7 cells per ml.

Table 1. ANT-300 dilution rates, with corresponding growth rates, and doubling times.

Dilution rate ^a $D \text{ (h}^{-1}\text{)}$	Growth rate $\mu \text{ (h}^{-1}\text{)}$	Doubling time $t_d \text{ (h)}$
$D = 0.015$	0.015	46.2
$D = 0.057$	0.057	12.2
$D = 0.170$	0.170	4.1
$D = 0.200$	0.200	3.5
Batch Culture ^b	0.144	4.8

^acells grown in continuous culture with SLX medium

^bcells grown with LIB-X medium

Cells from $D = 0.057 \text{ h}^{-1}$ (Fig. 2) began dropping in viability after approximately 21 days at a more gradual, but constant rate. Again, after 70 days of starvation, viability stabilized at nearly the same level as the $D = 0.015 \text{ h}^{-1}$ cell population and maintained viability in 0.3% of the total cell number.

Cells from $D = 0.170 \text{ h}^{-1}$ also lost their viability at a gradual and constant rate (Fig. 3). However, this began earlier than the $D = 0.015 \text{ h}^{-1}$ and $D = 0.057 \text{ h}^{-1}$ cells, at approximately 7 to 14 days. Once more after 70 days of starvation, viability stabilized at approximately 0.3% of the total cell number and maintained viable cells at the same levels as the cell populations from $D = 0.015 \text{ h}^{-1}$ and $D = 0.057 \text{ h}^{-1}$.

Cells from batch culture (Fig. 4) began to lose viability after approximately 21 days, but showed a significant drop (approximately two orders of magnitude) in the next 2 weeks. This was much faster than any of the other continuous cultured cell populations tested. Again, after 70 days of starvation, viability stabilized at approximately 0.3% of the total cell number.

The density of viable cells at approximately 10^5 cells per ml was maintained in each case throughout the remainder of the 98 day starvation period. Total cell numbers, with the exception of greater fluctuation at the onset, remained at constant cell density with approximately $2-3 \times 10^7$ cells

Fig. 1 Total cells, viable cells, and optical density
with starvation time for cells from
 $D = 0.015 \text{ h}^{-1}$.

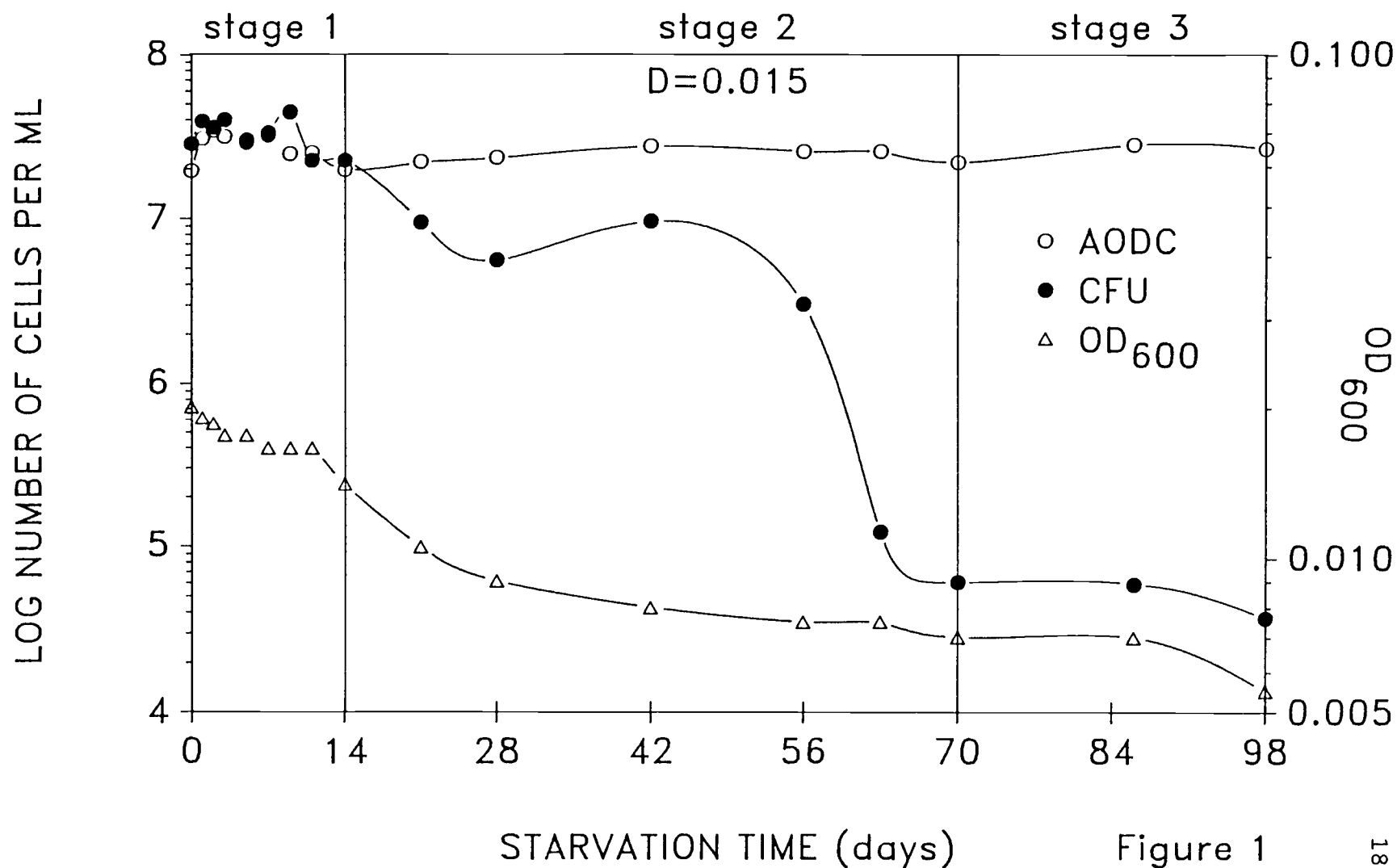


Figure 1

Fig. 2 Total cells, viable cells, and optical density
with starvation time for cells from
 $D = 0.057 \text{ h}^{-1}$.

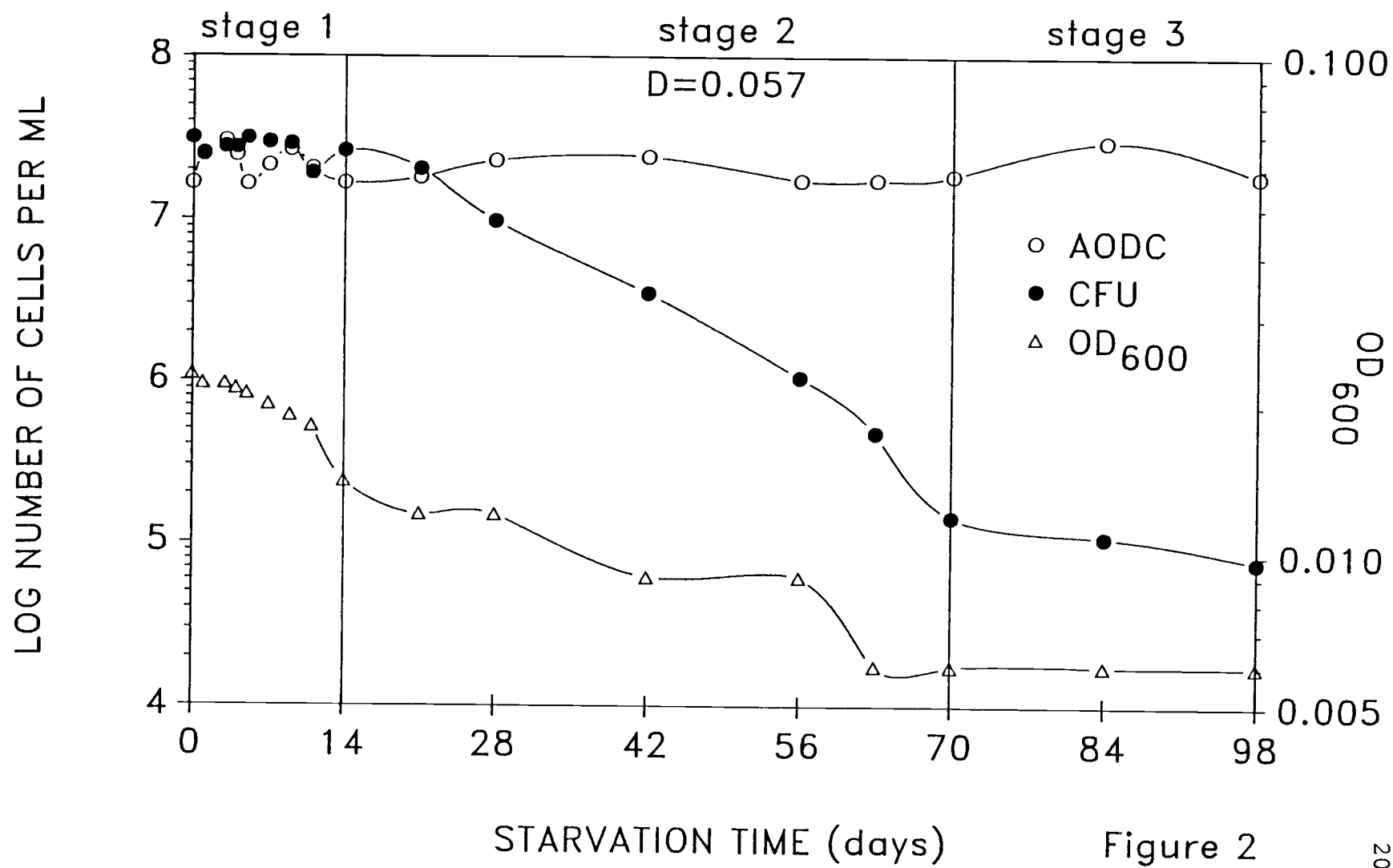


Figure 2

Fig. 3 Total cells, viable cells, and optical density
with starvation time for cells from
 $D = 0.170 \text{ h}^{-1}$.

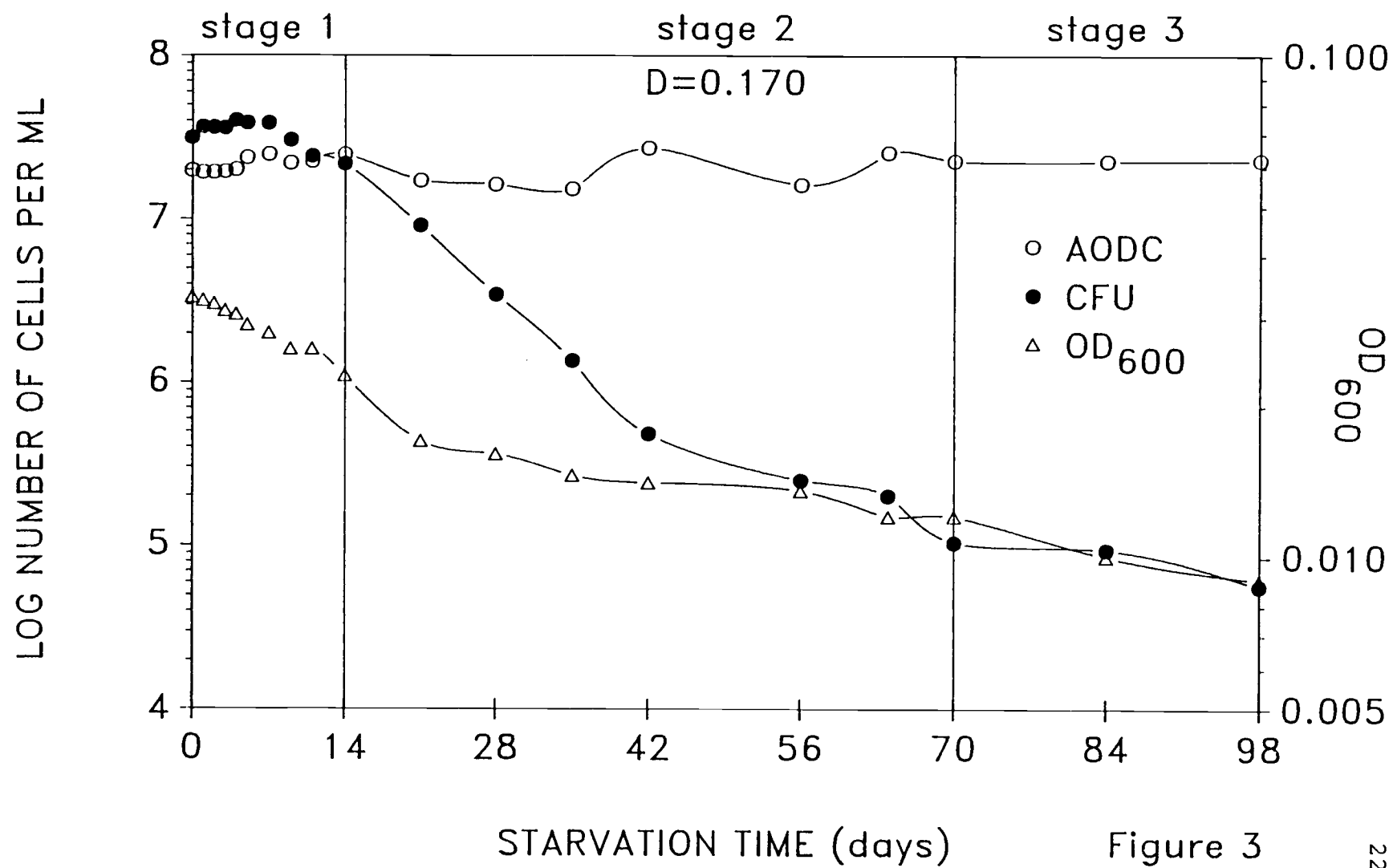


Fig. 4 Total cells, viable cells, and optical density
with starvation time for cells from batch
culture.

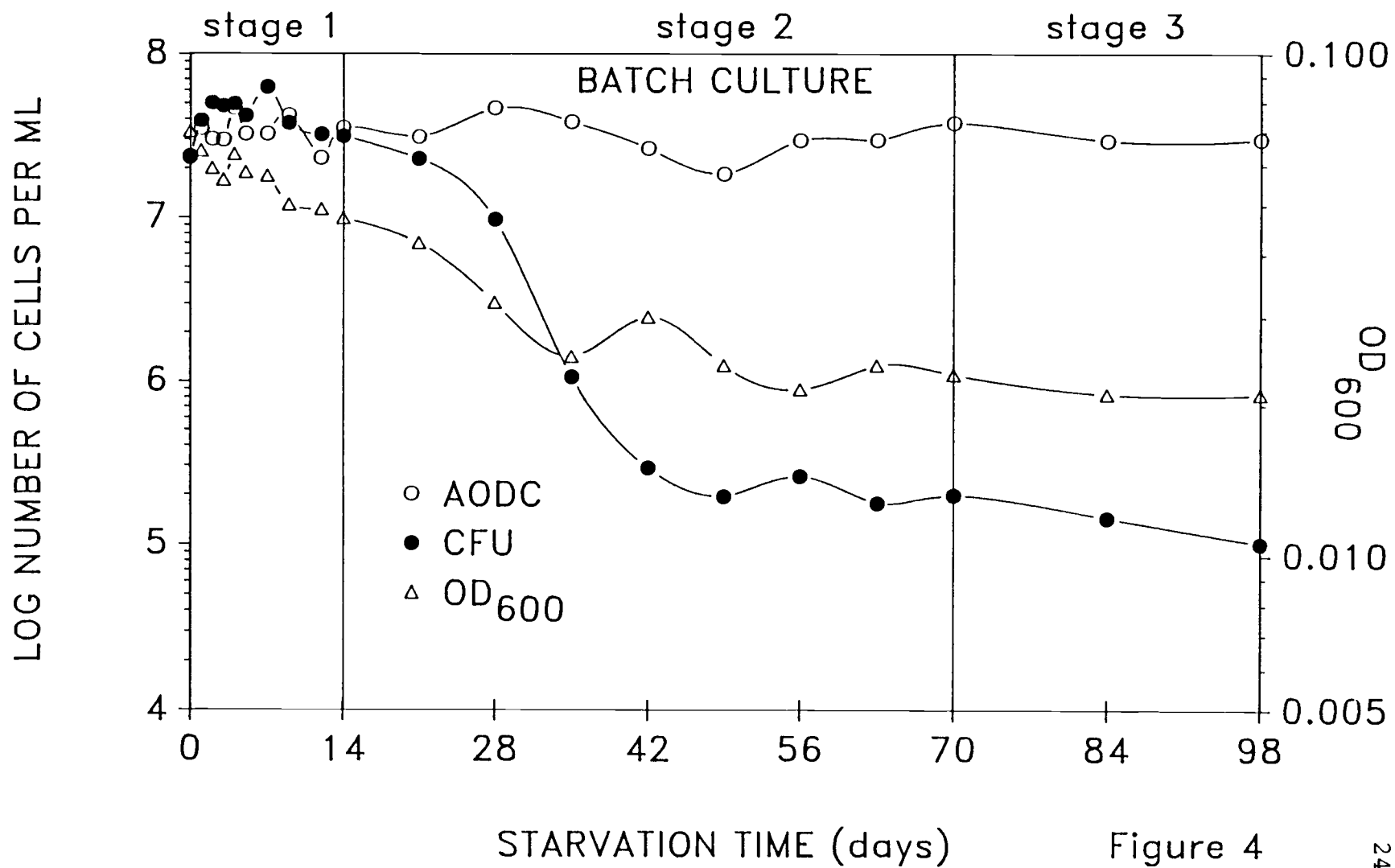


Figure 4

per ml showing no significant changes during the starvation period. In all cases, turbidity measurements indicated steady decreases in biomass, although the faster growing ($D = 0.170 \text{ h}^{-1}$ and batch culture) cells were able to maintain higher levels throughout the starvation-survival period. This is most likely due to a high amount of residual cellular material because of the fast growth rate or rich nutrient media, respectively.

Long-term starvation of a cell population grown at $D = 0.200 \text{ h}^{-1}$ (Fig. 5) showed a similar pattern to cells grown at $D = 0.170 \text{ h}^{-1}$ (Fig. 3), especially with respect to viability. After the initial decrease in viability which ended at approximately 70 days, a slower rate of decrease began. This extended starvation period which lasted 175 days, still ended with viable cells equalling approximately 0.3% that of the total cells. Once more, direct counts remained nearly constant throughout, indicating minimal cellular destruction.

The overall pattern from all these data indicates three separate stages of change occurring with respect to viable counts: (i) Large fluctuations with moderate overall decreases within the first 14 days. (ii) A 99.7% decrease, with the rate of viability loss depending upon the growth rate of the original cell population. (iii) The stabilization of the viable cell subpopulation after 70 days to approximately 10^5 cells/ml or 0.3% viability of

Fig. 5 Total cells, viable cells, and optical density
with starvation time for cells from
 $D = 0.200 \text{ h}^{-1}$.

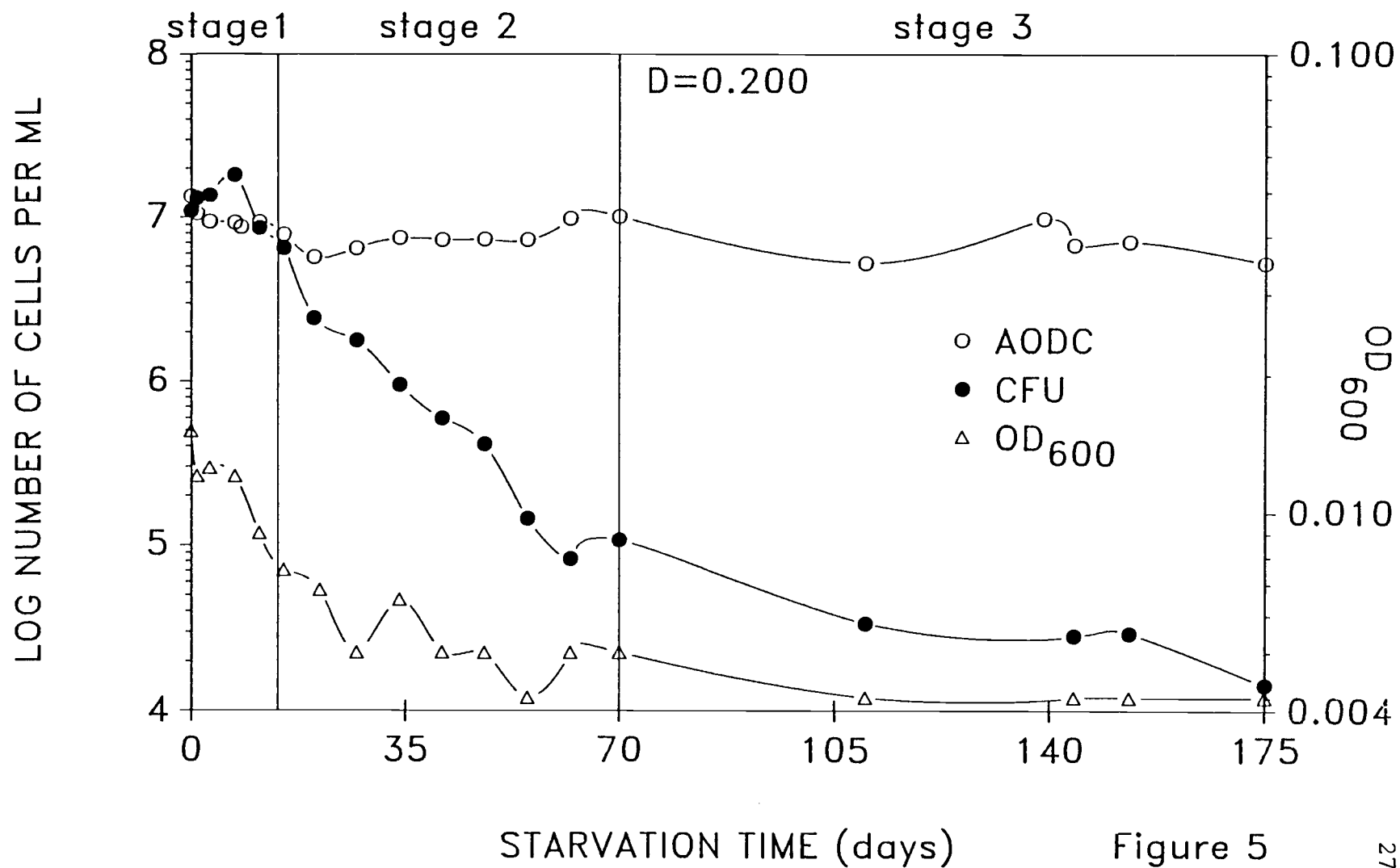


Figure 5

total cell numbers. These correspond to three distinct stages which can be defined as follows: stage 1 - from day 0 to day 14, stage 2 - from day 14 to day 70, and stage 3 - from day 70 to day 98 and beyond.

The duration of the three stages of starvation-survival need not be identical for other marine bacteria. However, the existence of the three stages do seem to be present in other species. The viability of a marine Pseudomonad sp. was found by Kurath (1983) to have an initial increase lasting for 5 days, corresponding to the duration of stage 1. In the same study, viability dropped to 0.1% of that of the total population after just 25 days, corresponding to stage 2. After this, viability stabilized for the remainder of the 40 day starvation period, corresponding to stage 3.

The rate of viability loss during stage 2 indicates that survivability is dependent on the growth rate of the cell source population. Cells grown at $D = 0.015 \text{ h}^{-1}$ show that their viability is extended relative to the other cell populations. The viable cell counts did not begin to significantly drop until approximately day 56 of starvation-survival. At this time an accelerated drop in viability of over 2 orders of magnitude to 0.3% of the total cell level occurred prior to the culmination of stage 2. This is markedly different from the viability pattern seen for ANT-300 cell populations originally from

faster growth rates during the starvation period.

Cell populations originally grown at $D = 0.057 \text{ h}^{-1}$ and $D = 0.170 \text{ h}^{-1}$ were similar in that they both demonstrated steady rates of decrease from early stage 2. However, they did differ in that cells grown at $D = 0.057 \text{ h}^{-1}$ were able to sustain their viability counts 7-14 days longer before the steady rate of viability decrease began. Cells from both growth rates eventually dropped in viability to approximately 0.3% of the total cell level. Cells originating from logarithmic growth in batch culture showed a pattern that was opposite of that found in $D = 0.015 \text{ h}^{-1}$ cells. These cells showed a significant decrease in viability early in stage 2, dropping to nearly the 0.3% level of viability within 28 days and stabilizing at that level for the remainder of the starvation period.

Once 70 days of starvation-survival has been reached (stage 3), the stabilization of viability for each of the cell populations, relative to total cell counts (Fig. 1-5), indicates that the stabilization of certain cellular processes are common to all cell populations during starvation-survival regardless of the original growth rate. This stabilization is presumed to be due to the metabolic arrest as hypothesized by Morita (1988) to occur during starvation-survival. As will be shown later in this thesis, similar stabilization patterns were observed in DNA, RNA, and protein concentrations on either a total cell

(Fig. 8-11) or viable cell (Fig. 12-15) basis.

Biovolume Assessment

Biovolumes for the cells from each cell population were determined for unstarved and starved cells (Fig. 6 and 7). The cell volumes are summarized in Table 2. Unstarved $D = 0.200 \text{ h}^{-1}$ cell volume was omitted because it was assumed to have approximately the same cellular volume as unstarved $D = 0.170 \text{ h}^{-1}$ cells. Unstarved logarithmically grown cells (labeled LOG in Fig. 6 and 7) at nearly $6 \mu\text{m}^3$ in cell volume, were much larger than any other ANT-300 cell population because they were grown in rich medium (LIB-X). The unstarved ANT-300 cells grown in continuous culture became smaller with decreasing dilution rates, with a decrease in volume from $1.16 \pm 0.156 \mu\text{m}^3$ at $D = 0.170 \text{ h}^{-1}$, $0.585 \pm 0.038 \mu\text{m}^3$ at $D = 0.057 \text{ h}^{-1}$, and $0.478 \pm 0.060 \mu\text{m}^3$ at $D = 0.015 \text{ h}^{-1}$ (Fig. 6).

The length of starvation time is shown in Fig. 7, along with the respective cell volumes for the starved cells from each of the ANT-300 cell populations examined. Cells from the $D = 0.015 \text{ h}^{-1}$ population were significantly lower in volume at $0.046 \pm 0.010 \mu\text{m}^3$ than any of the other cell volumes. However, these cells were starved 95 days less than the cells from $D = 0.200 \text{ h}^{-1}$ which maintained their volume at $0.258 \pm 0.030 \mu\text{m}^3$ after almost 1 year of starvation.

Table 2. Biovolume measurements for starved and unstarved ANT-300 cells.

Dilution rate ^a D (h ⁻¹)	Cell volume (μm ³)	
	Unstarved	Starved ^c
Batch Culture ^b	5.94 ± 0.465	0.275 ± 0.053
D = 0.170	1.16 ± 0.156	0.189 ± 0.030
D = 0.057	0.585 ± 0.038	0.181 ± 0.033
D = 0.015	0.478 ± 0.060	0.046 ± 0.010
D = 0.200	-----	0.258 ± 0.030

^acells grown in continuous culture with SLX medium

^bcells grown with LIB-X medium

^cCells from stage 3

Throughout the starvation-survival period there was a general decrease in biomass as determined by OD₆₀₀ measurements (Fig. 1-5). Biovolume measurements also showed this decrease to occur with the starvation of any one cell population. The ANT-300 cells decreased in volume significantly during starvation-survival, which in turn increases their surface to volume ratio. Regardless of starvation time however, it was demonstrated that biovolume was dependent upon the original growth rate more than the length of time starved. This is a very critical point if one desires to study the starvation-survival of bacteria which are representative of those in the marine environment. The cells, which were by far the smallest in volume at $0.046 \pm 0.010 \mu\text{m}^3$, originally came from the slowest grown cell population ($D = 0.015 \text{ h}^{-1}$). These cells were starved a total of 251 days. This contrasts with the cells grown at $D = 0.200 \text{ h}^{-1}$ which were $0.258 \pm 0.030 \mu\text{m}^3$ and had been starved 352 days (95 days longer than the $D = 0.015 \text{ h}^{-1}$ cells). Therefore, these data indicate that cells which are greater in surface to volume ratios at the beginning of starvation-survival are able to maintain greater surface to volume ratios throughout the entire starvation-survival period. This suggests that the $D = 0.015 \text{ h}^{-1}$ cells would be better adapted to the survival of long-term starvation than the other cell populations. Another important fact, brought forth by these studies, is

Fig. 6 Biovolume of unstarved cells. Cell populations sampled were as follows: Batch culture (labeled LOG), $D = 0.170 \text{ h}^{-1}$, $D = 0.057 \text{ h}^{-1}$, and $D = 0.015 \text{ h}^{-1}$. The hatched bars represent the mean of 20 cell volume determinations from each population; the vertical bars represent the standard error of the mean.

BIOVOLUME OF UNSTARVED CELLS

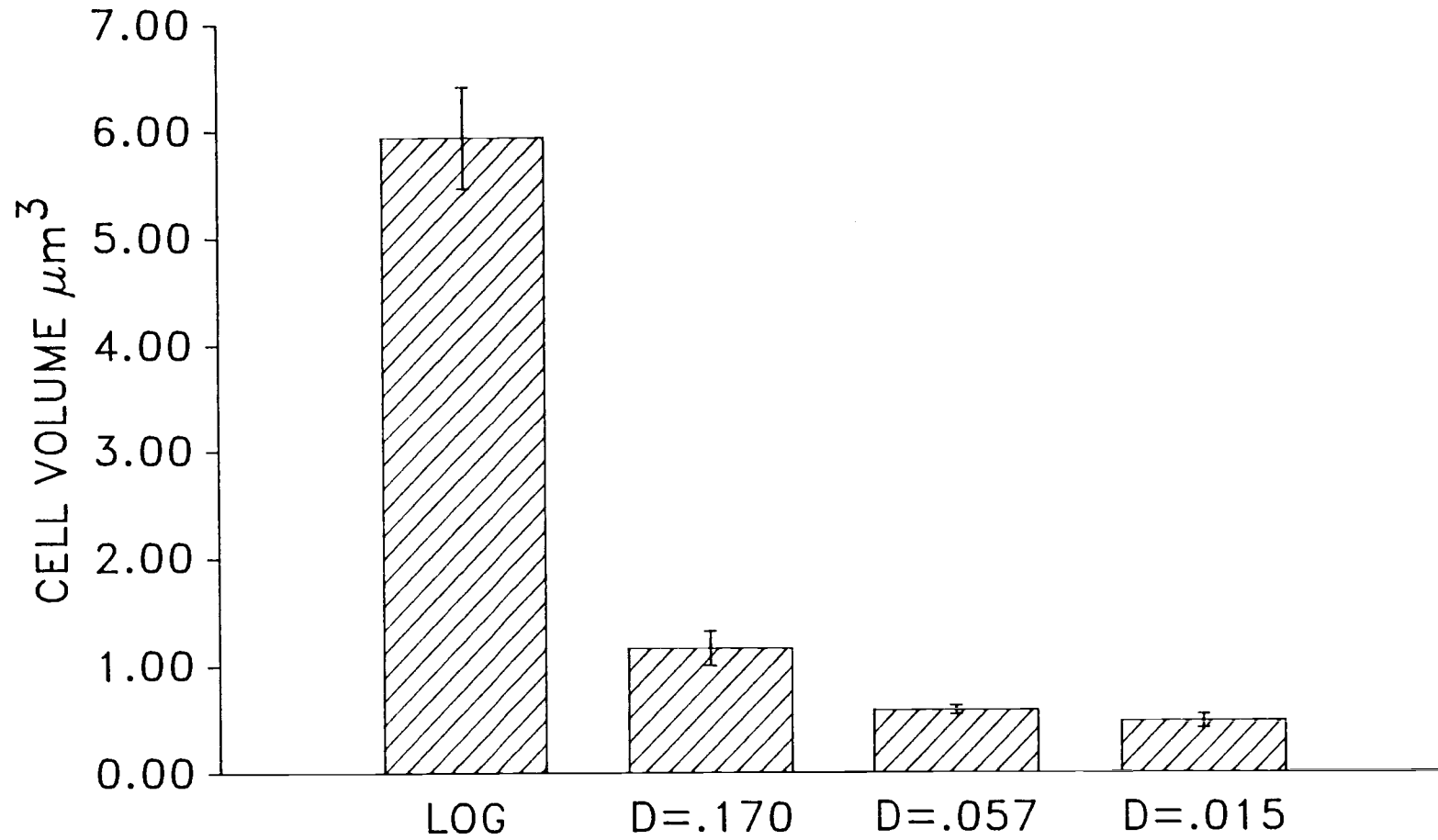


Figure 6

Fig. 7 Biovolume of starved cells. Cell populations sampled were as follows: Batch culture (labeled LOG) starved 195 days, $D = 0.170 \text{ h}^{-1}$ starved 231 days, $D = 0.057 \text{ h}^{-1}$ starved 248 days, $D = 0.015 \text{ h}^{-1}$ starved 259 days, and $D = 0.000 \text{ h}^{-1}$ starved 354 days. The hatched bars represent the mean of 20 cell volume determinations from each population; the vertical bars represent the standard error of the mean.

BIOVOLUME OF STARVED CELLS

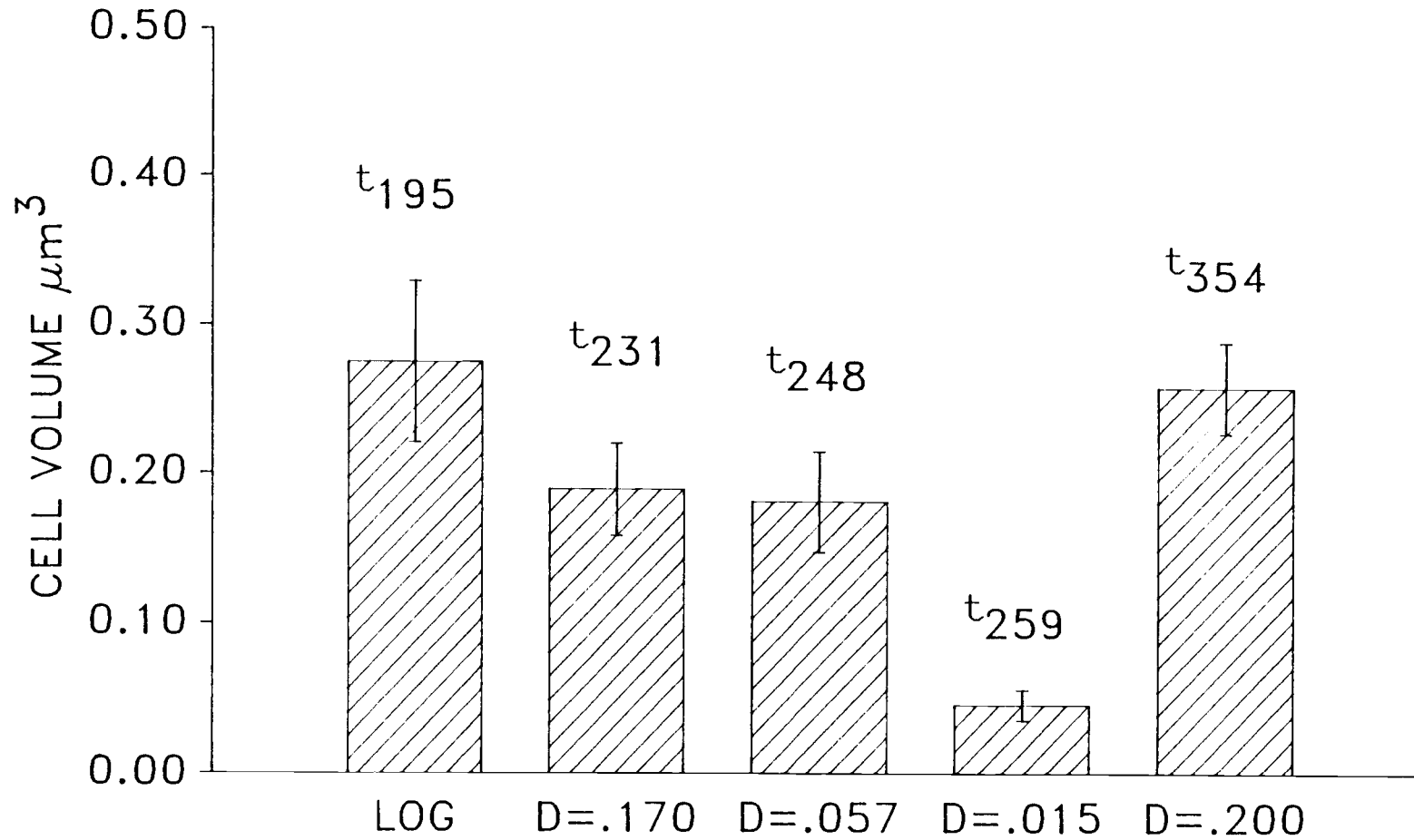


Figure 7

that cells do not have to become large (i.e., Log cell size, Fig. 6) before they divide. This brings up the question as to how large a cell must be before division can take place?

Macromolecular Fluctuations

For the duration of the starvation-survival period the concentrations of the macromolecules (DNA, RNA, and protein) were monitored on a per total cell basis (Fig. 8-11) and a per viable cell basis (Fig. 12-15). During initial starvation-survival period, DNA, RNA, and protein normalized to direct cell counts showed similar patterns of wide fluctuations. This corresponds to stage 1 of the starvation-survival period. The concentration levels of all three of the macromolecules within stage 1 showed 2-3 characteristic peaks. During stage 2 each of the populations showed DNA levels which steadily dropped on a per total cell basis and then stabilized at approximately 42-56 days, RNA concentrations remained higher than DNA, and with exception of the $D = 0.015 \text{ h}^{-1}$ cells, followed the fluctuations in protein concentration very closely. However, it should be noted that for the faster growing cells derived from $D = 0.170 \text{ h}^{-1}$ and batch culture (Fig. 10 and 11) the concentration scale for proteins was up to approximately 4 times higher than that of the total cells for $D = 0.015 \text{ h}^{-1}$ and $D = 0.057 \text{ h}^{-1}$ (Fig. 8 and 9) during

Fig. 8 DNA, RNA, and protein per total cell with
starvation time for cells from $D = 0.015 \text{ h}^{-1}$.

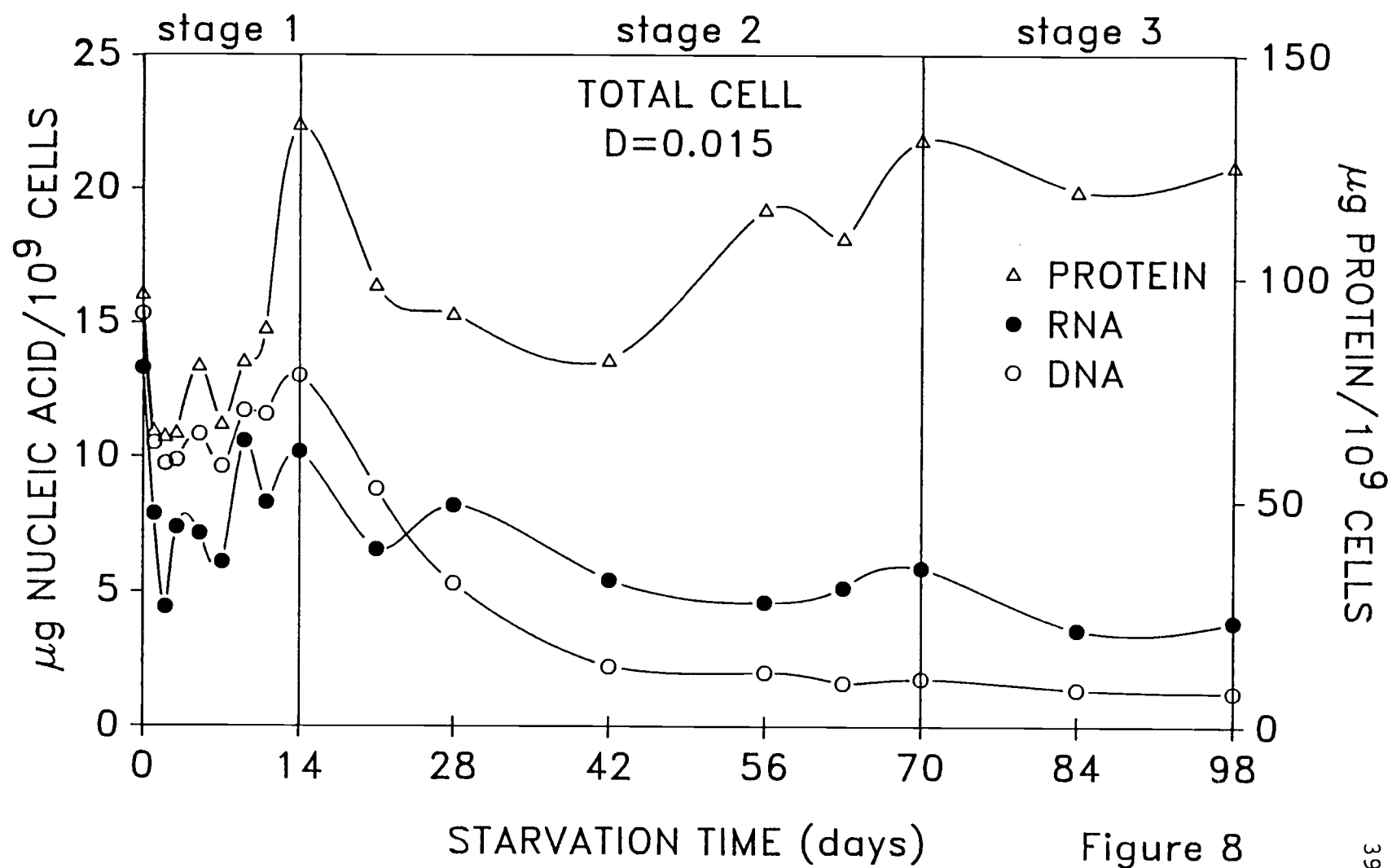


Figure 8

Fig. 9 DNA, RNA, and protein per total cell with
starvation time for cells from $D = 0.057 \text{ h}^{-1}$.

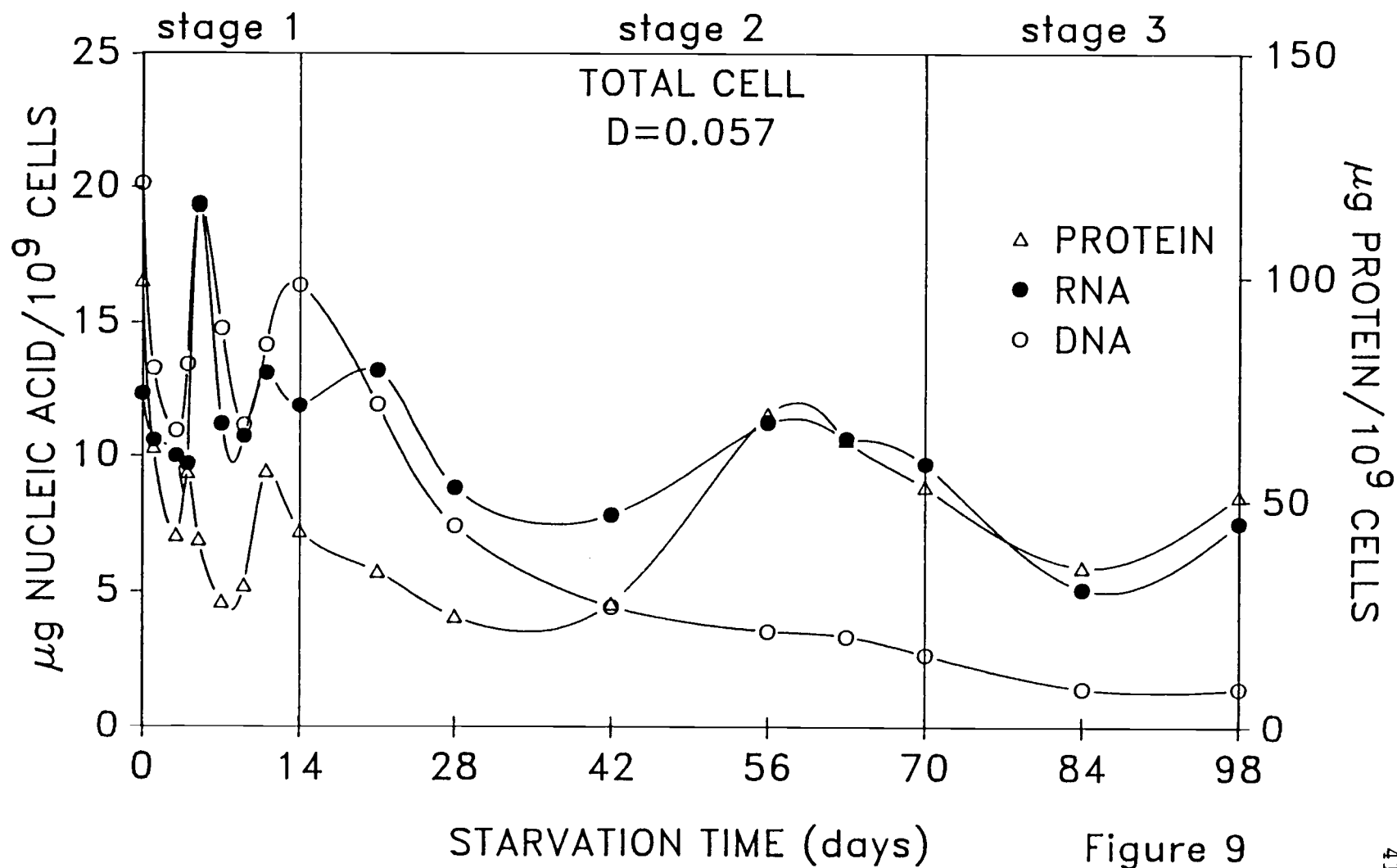


Figure 9

Fig. 10 DNA, RNA, and protein per total cell with
starvation time for cells from $D = 0.170 \text{ h}^{-1}$.

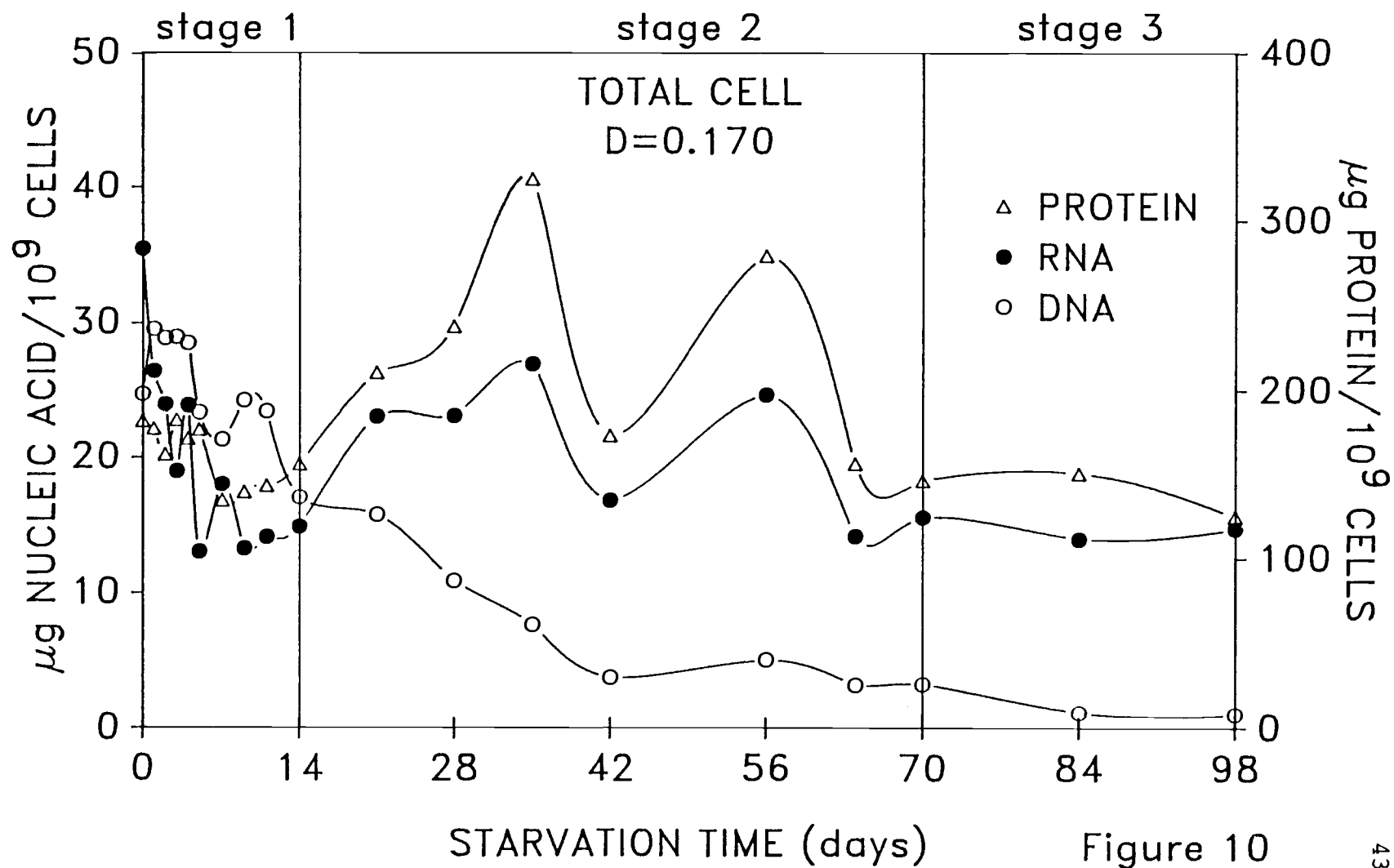


Figure 10

Fig. 11 DNA, RNA, and protein per total cell with
starvation time for cells from batch culture.

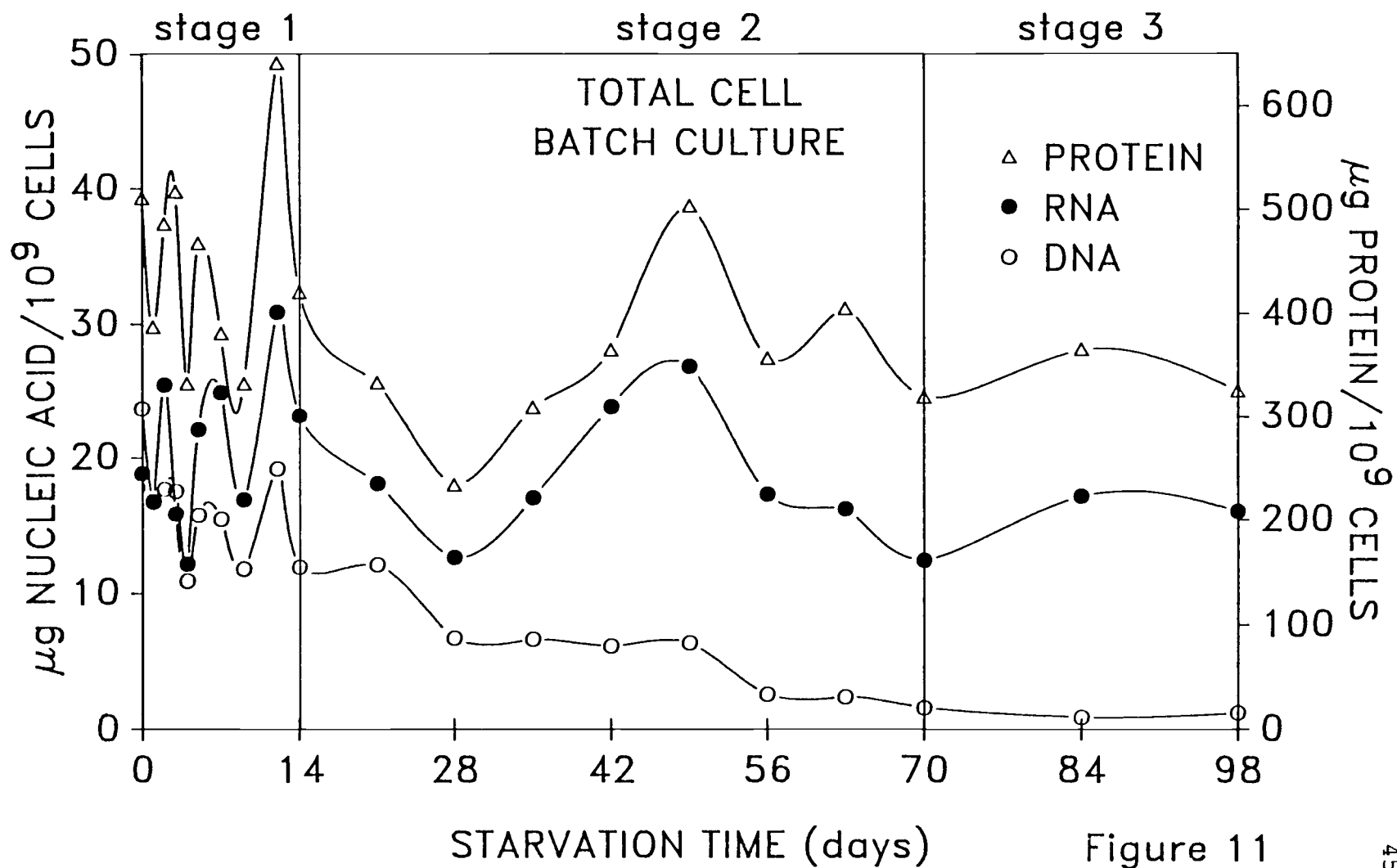


Figure 11

the entire 98 day period of starvation. During stage 2 it was also observed that protein concentrations (Fig. 8-11) after initially dropping, increased. Once the protein concentration per total cell began to rise there were two characteristic fluctuations which occurred for each of the different cell populations during stage 2. Finally, stage 3 shows an overall stabilization in DNA, RNA, and protein concentrations for all cell populations.

Over the course of starvation-survival, Ant-300 batch culture cells showed significant decreases in DNA per cell. Only 5.2% of the original DNA per total cell remained after 98 days of starvation. The RNA and protein per cell decreased overall, fluctuating heavily during stage 1, less during the stage 2, and finally stabilizing during stage 3. However, unlike the DNA per cell, RNA and protein per cell for the batch culture cell population decreased minimally to 85.0% and 63.7% of the original RNA and protein per cell, respectively, at the end of the 98 day starvation period. The cells from $D = 0.170 \text{ h}^{-1}$ showed an overall decrease in DNA to 4.2%, RNA to 41.4%, and protein to 68.6%. The cells from $D = 0.057 \text{ h}^{-1}$ showed an overall decrease in DNA to 7.2%, RNA to 61.1%, and protein to 51.6%. The $D = 0.015 \text{ h}^{-1}$ cells also demonstrated a drop in DNA per cell to 8.3% after 98 days of starvation. However, the RNA per cell dropped steadily after stage 1 to only 29.2% of the original concentration, and the protein per

cell increased to 129.7% that of the original concentration. This shows an overall protein production on a per cell basis.

The concentrations of DNA, RNA, and protein showed similar fluctuation patterns during stage 1 of starvation-survival. The characteristic 2-3 major peaks with respect to the concentration of each of the macromolecules was observed for each of the cell populations examined, and was monitored on both a total cell (Fig. 8-11) and viable cell basis (Fig. 12-15). The fluctuations which took place during stage 1 occurred with greater magnitude and periodicity than any others seen throughout the rest of starvation-survival. This indicates a redistribution of cellular constituents primarily during stage 1 which prepares the cells for long-term starvation-survival. Marden et al. (1985) demonstrated that a period of metabolic shut down occurs, where exchanges with the environment are reduced as displayed by decreased oxygen uptake, but that an initial energy dependent reorganization which involves an increased endogenous respiration occurs in the unclassified marine isolate S14. Marden et al. (1988) also observed bacterial DNA synthesis to occur during the first few hours of starvation for various marine isolates. Overall, this process represents a metabolic adjustment which leads to the cellular adjustment of the macromolecules DNA, RNA, and protein. During starvation,

the cells must rely on internal energy reserves as the sole energy supply. Evidence in support of this is shown by Hood et al. (1986) who starved Vibrio cholerae and found that its entire reserves of poly- β -hydroxybutyrate were utilized by day 7 of starvation-survival. The poly- β -hydroxybutyrate reserves were utilized faster in marine isolate S14, and could not be detected after only 3 h when S14 was starved under complete energy and nutrient depleted conditions (Malmcrona-Friberg et al., 1986). Changes in the fatty acid profile of starved V. cholerae cell membrane have been demonstrated to occur within 7 days (Guckert et al., 1986). It is possible that the high degree of fluctuation in macromolecule concentrations, especially seen on a total cell basis, is representative of switching metabolism towards nutrient scavenging. This has also been observed through the production of high affinity uptake systems (Geesey and Morita, 1979) and increased chemotaxis (Torrella and Morita, 1982) in ANT-300.

After the initial transition period, the cells entered stage 2, which was a period where the fluctuations of intercellular constituents were buffered from any drastic changes due to the decrease in metabolic activity. Endogenous metabolism for ANT-300 has been shown to decrease to 0.0071% total carbon respired per h after 7 days and to remain constant thereafter (Novitsky and Morita, 1977). The endogenous metabolism of another marine

Vibrio sp., strain DW1, has been shown to drop during initial starvation-survival to 58% after 5 h and 6% after 5 days via oxygen uptake measurements (Kjelleberg et al., 1982). It is during this period that the metabolism slows to a point which leaves the cell unable, or with limited ability to, catabolize macromolecules, such as DNA, RNA, or protein. This is most likely due to the lack of usable carbon, which is quickly exhausted. It is also during stage 2 when the viability of cells diminishes to only 0.3% of that of total cell numbers and remains there for the duration of starvation-survival. The fact that the total cell numbers maintain close to original levels indicates that the cells are not lysing with the onset of starvation-survival, but remaining in a state of metabolic arrest as postulated by Morita (1988) which allows them to survive extremely long periods of time without further nutrient input, i.e. stage 3 starvation-survival.

The peaks in protein and RNA per cell as demonstrated by all the populations of ANT-300 during mid to late stage 2 of the starvation period as well as the stage 3 elevated protein levels of the $D = 0.015 \text{ h}^{-1}$ cell population, may represent the production of starvation resistant proteins. Starvation proteins for ANT-300 have been demonstrated by Amy and Morita (1983) to occur only after a sufficient starvation period has elapsed. The synthesis of starvation proteins has also been observed for

Escherichia coli (Grout and Matin, 1986) and three marine isolates, including the marine Vibrio sp. DW1 (Jaan et al., 1986).

Throughout the starvation-survival period, concurrent fluctuations of RNA and protein concentrations per cell were observed, and DNA per cell dropped steadily to 5-10% of the original concentration, regardless of the original growth rate of the cell population. This corresponds to the DNA level stabilizing at ca. 1.0 - 1.5 fg DNA per total cell for all cell populations during stage 3. The decrease in cellular DNA may be due to the cells reducing DNA content to a one copy of each gene or at least to the necessary DNA required to maintain functional during the metabolic arrest state of stage 3. This DNA must also allow for growth initiation and reproduction when conditions permit. The concentration of protein and RNA per total cell is closely coupled through stages 2 and 3 for all cell populations examined, except for $D = 0.015 \text{ h}^{-1}$. These uncouple early at the beginning of stage 2, where the RNA per cell decreases much like the DNA per cell and protein per cell continues the increase to the beginning of stage 3 when stabilization occurs. Since RNA per cell for the $D = 0.015 \text{ h}^{-1}$ cells decreased significantly relative to protein, it is hypothesized that these proteins were translated from ribosomes (the most abundant stable form of RNA) that were more efficient at

protein production under a reduced metabolic state. It is proposed that ribosomal efficiency is what increases due the lack of energy that would "normally" be required for translation under nutrient rich conditions. Therefore, it is postulated that not only proteins can switch over to higher affinities i.e. efficiency with starvation, but that RNA can function in this manner as well. This is in contrast to the inefficiency of ribosomes in bacteria with doubling times less than 2 h, as stated by Koch (1980). It is also in contrast with the concept of "extra RNA" as proposed by Koch (1971), which is said to occur in slow growing bacteria because of the energetically expensive nature of these molecules (Koch, 1985). These differences are most likely due to the work of Koch being done with E. coli, which is normally a fast growing bacterium.

As discussed earlier, the protein concentration for the $D = 0.0170 \text{ h}^{-1}$ and batch culture populations are up to 4 times higher than that of the other cell populations (Fig. 10 and 11). These data indicate that the cells from $D = 0.170 \text{ h}^{-1}$ and batch culture had to contend with elevated protein concentrations during starvation-survival, but had insufficient energy for their utilization. Koch (1971 and 1979) has found that E. coli is not capable of degrading certain classes of proteins under similar conditions, which may also apply for marine bacteria. Therefore, because these cell populations were apparently

Fig. 12 DNA, RNA, and protein per viable cell with
starvation time for cells from $D = 0.015 \text{ h}^{-1}$.

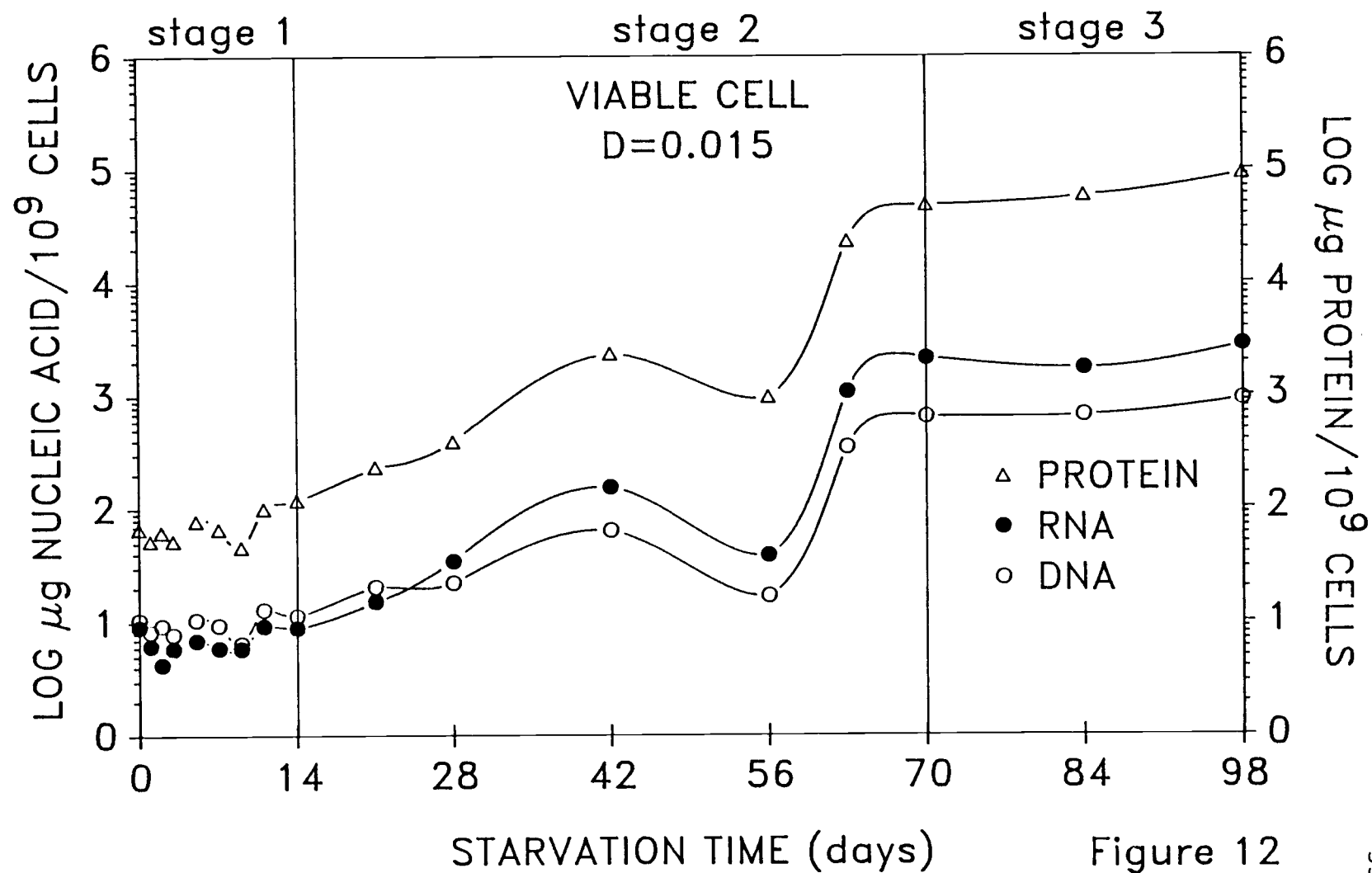


Figure 12

Fig. 13 DNA, RNA, and protein per viable cell with
starvation time for cells from $D = 0.057 \text{ h}^{-1}$.

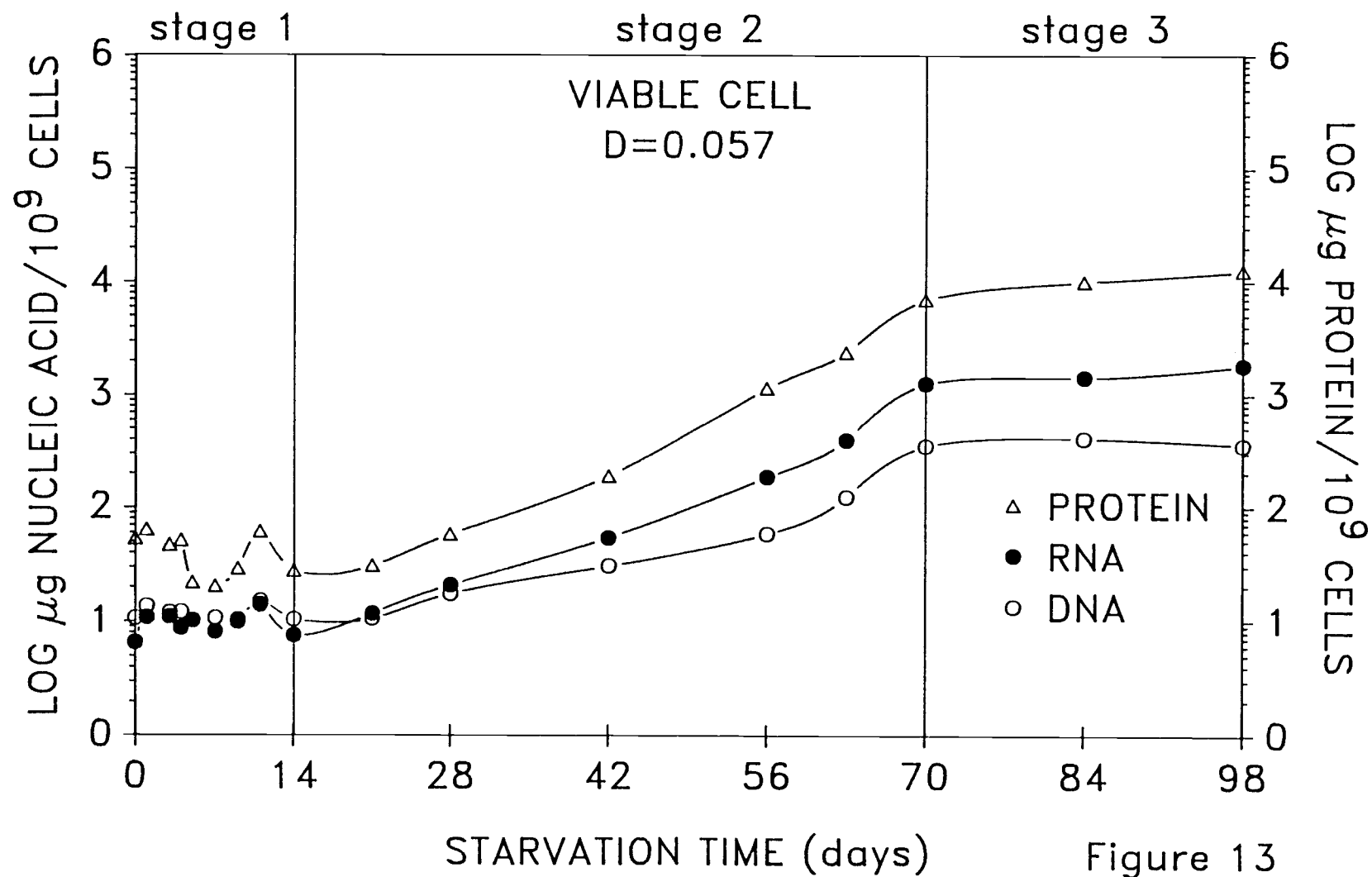


Figure 13

Fig. 14 DNA, RNA, and protein per viable cell with
starvation time for cells from $D = 0.170 \text{ h}^{-1}$.

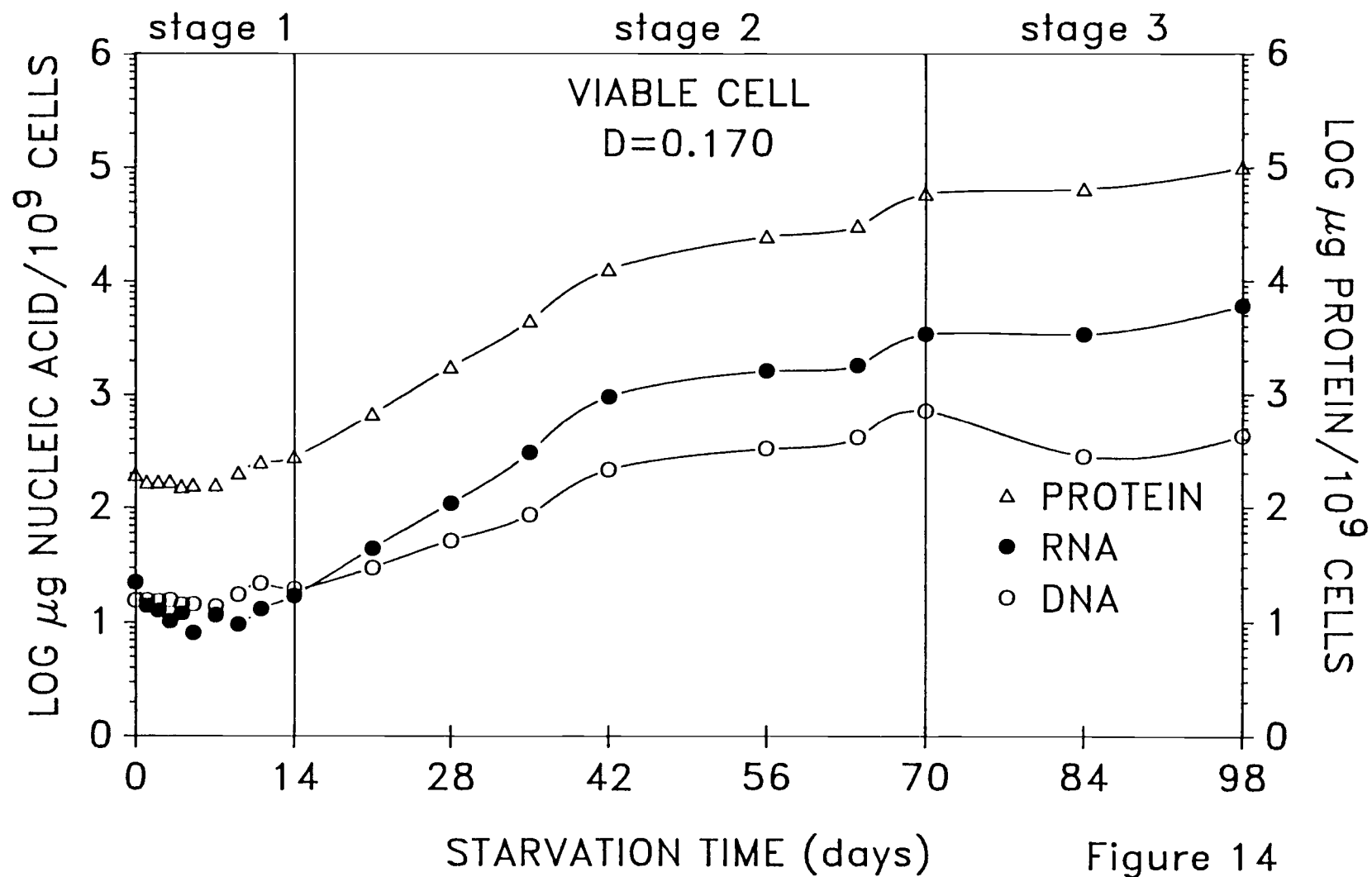


Figure 14

Fig. 15 DNA, RNA, and protein per viable cell with
starvation time for cells from batch culture.

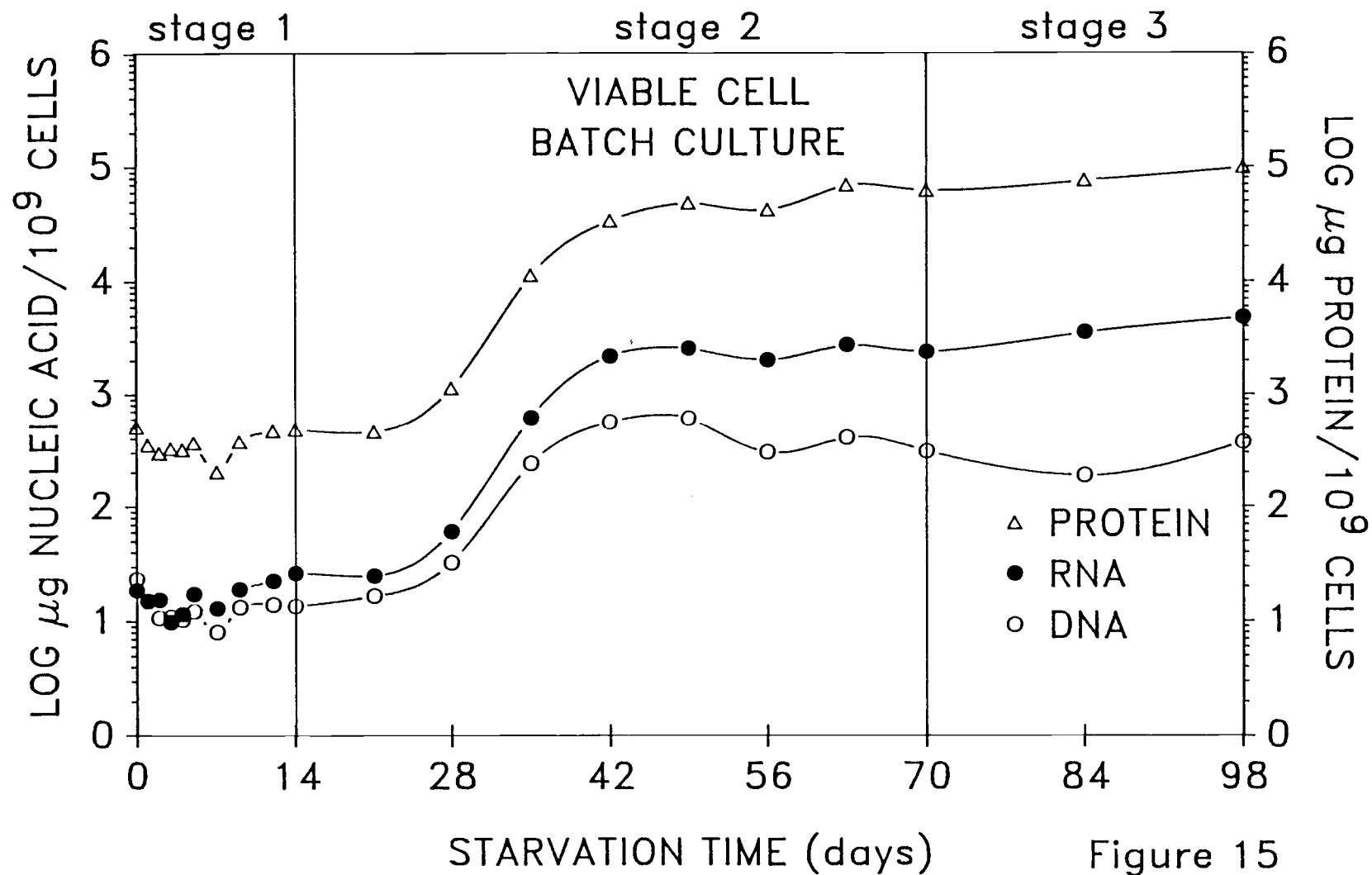


Figure 15

unable to degrade the high levels of protein acquired from fast growth and rich media, respectively, high residuals of protein were observed throughout all three stages of starvation-survival.

All three stages of starvation-survival showed reproducible patterns of DNA, RNA, and protein concentrations normalized to viable cells (Fig. 12-15). Once again, stage 1 showed a high degree of fluctuation with 2-3 characteristic DNA, RNA, and protein peaks in each population. During stage 2, concentrations of all macromolecules increased 2-3 fold. The large overall increases in macromolecule concentration reflect a bias due to the magnitude of losses in viable cells especially during stage 2 for each of the cell populations examined. Stage 3 showed a stabilization for each of the macromolecule concentrations with respect to viable cells in each of the populations. These results are influenced by the inability to separate the viable cells from dead or dormant cells in each population. However, intact cells would most likely retain most of their macromolecules (Amy, 1982, Ph.D. thesis, Oregon State University). Therefore, the data for concentrations of macromolecules in total cells are considered to have the highest accuracy. Overall, the cells from each of the populations are remaining intact throughout the starvation period helping to support the validity of this assumption.

DNA Electron Micrographs

In addition to the quantification that DNA levels drop during starvation-survival, unstarved and starved cellular DNA was also qualitatively analyzed by electron micrographs (Fig. 16). The cellular DNA from unstarved cells logarithmically grown in batch culture is presented in Fig. 16A and 16B. The cellular DNA from cells grown using the same method, and which were starved 98 days, is presented in Fig. 16C and 16D. The latter DNA molecules are significantly smaller in size, demonstrating the loss of DNA which occurs during starvation-survival. These data show a reduction in the actual cellular DNA molecule, supporting the hypothesis that the cell reduces its DNA to single functional genome, as discussed earlier.

Macromolecule Ratios

The ratios of DNA, RNA, and proteins have been included to demonstrate the relationships between macromolecule concentrations (Fig. 17-22). DNA/RNA ratios (Fig. 17) again showed three separate stages of starvation-survival, with the onset of heavy fluctuation and the characteristic 2-3 major peaks, followed by an overall decline, and then finally stabilization. These corresponded respectively to stages 1, 2, and 3. In cell populations examined, DNA levels per cell dropped. This was seen in the overall decreasing DNA/RNA ratio curves

Fig. 16 Electron micrographs of the DNA molecule from logarithmic growth unstarved (A and B) and 98 day starved (C and D) cells. The bar represents one micrometer.

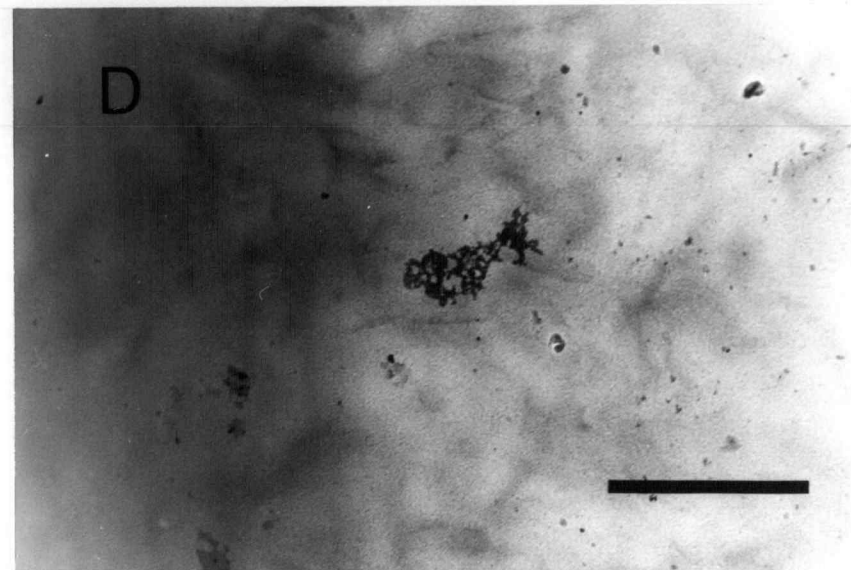
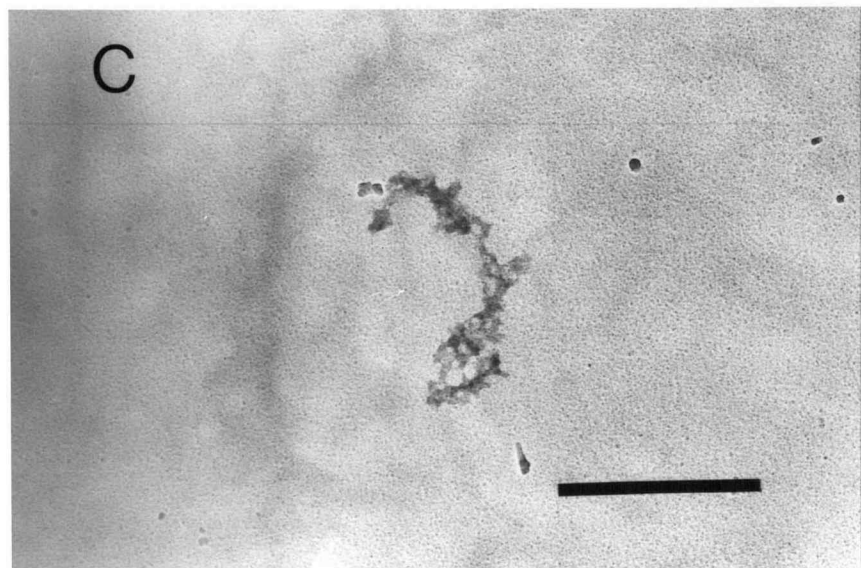
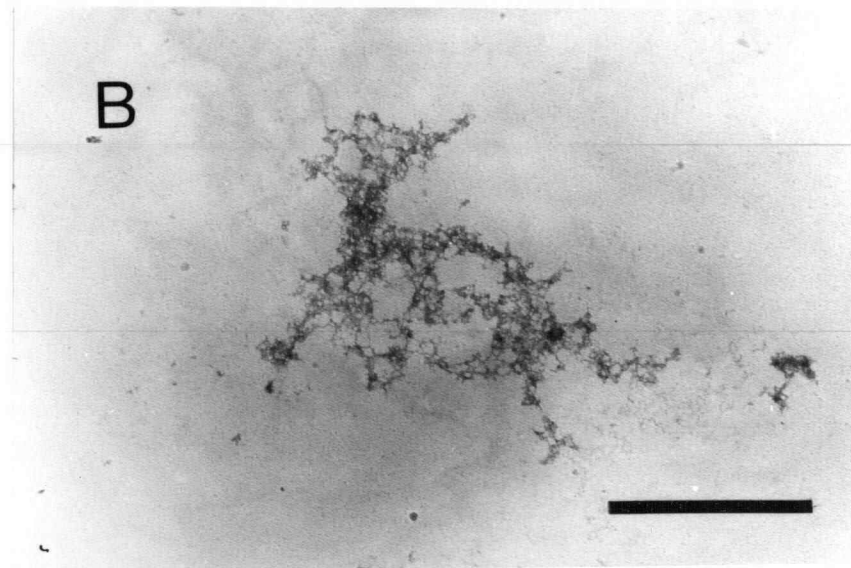
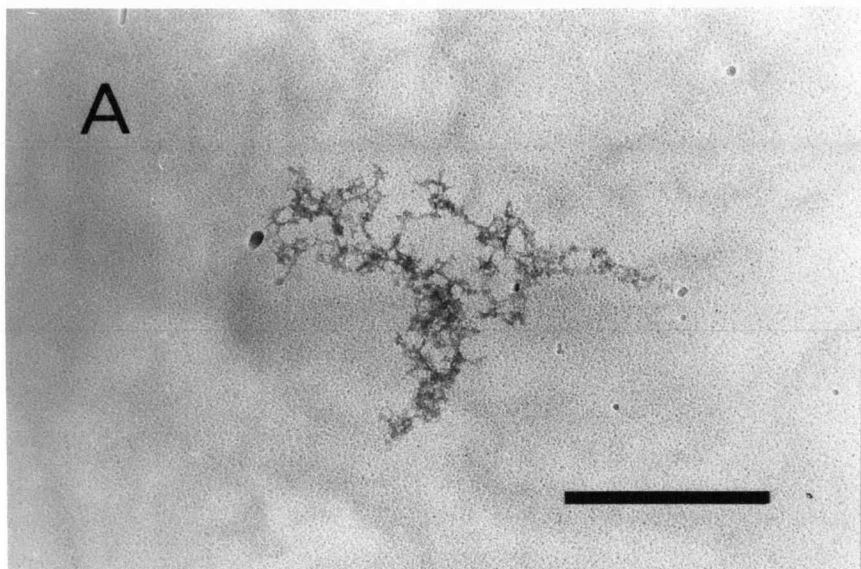


Fig. 17 DNA/RNA ratios with starvation time. Calculated for the following cell populations: Batch culture, $D = 0.170 \text{ h}^{-1}$, $D = 0.057 \text{ h}^{-1}$, and $D = 0.015 \text{ h}^{-1}$.

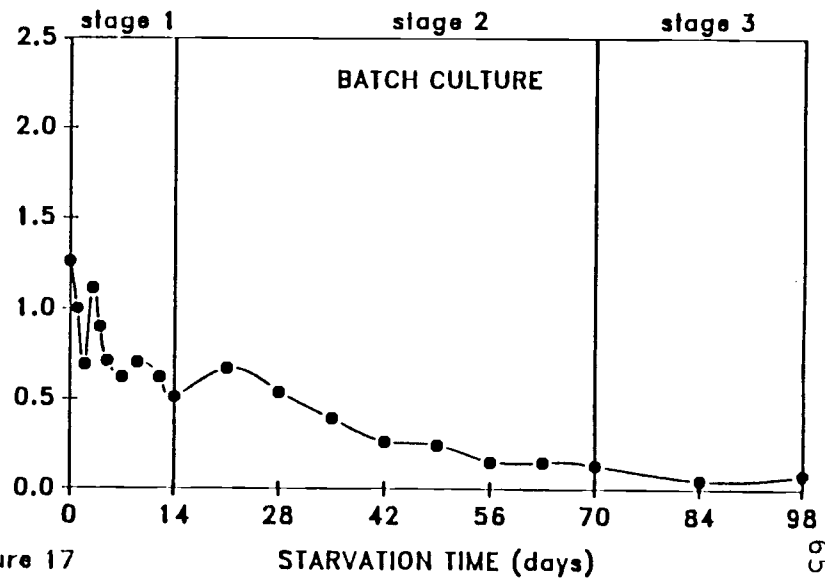
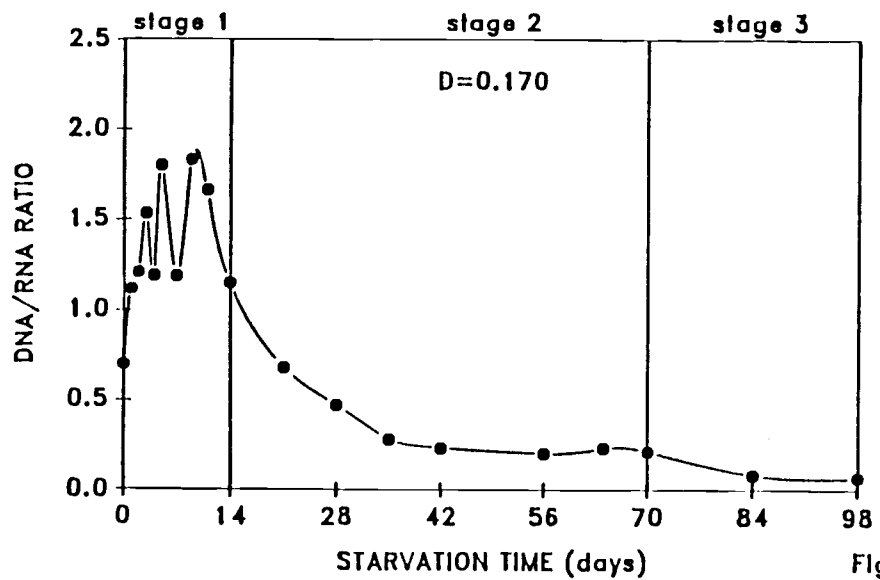
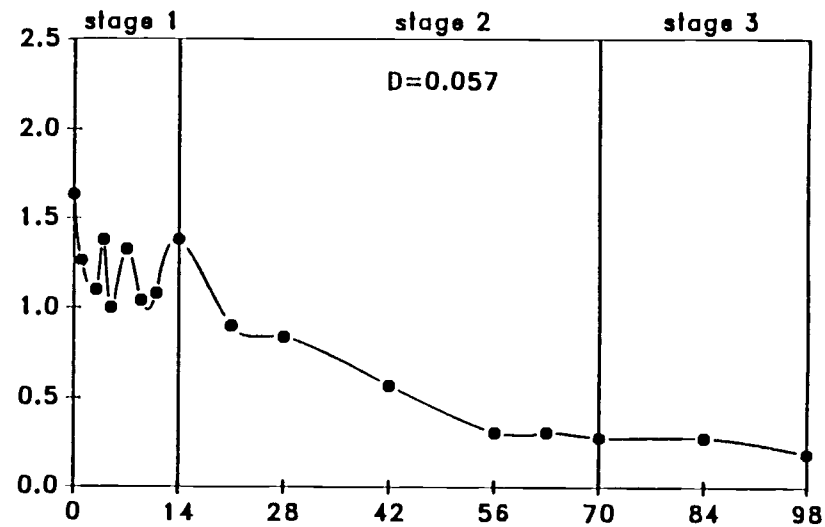
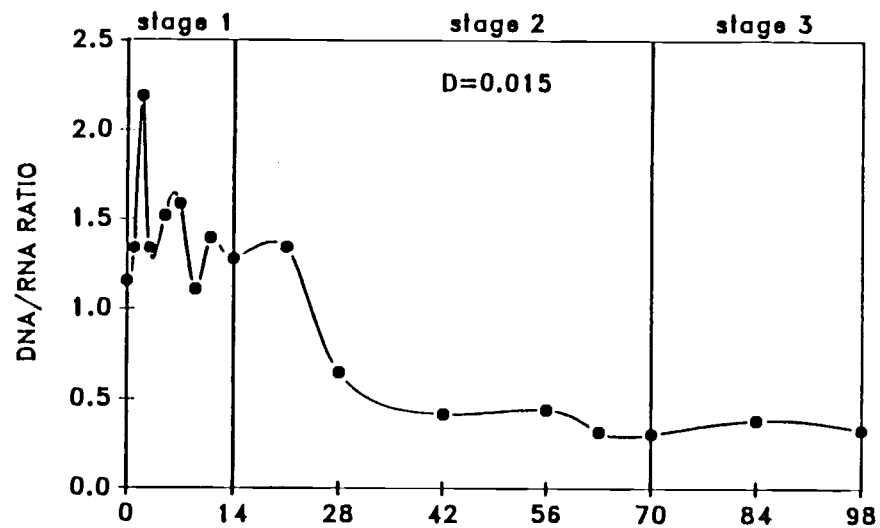


Figure 17

Fig. 18 DNA/protein ratios with starvation time.
Calculated for the following cell populations:
Batch culture, $D = 0.170 \text{ h}^{-1}$, $D = 0.057 \text{ h}^{-1}$, and
 $D = 0.015 \text{ h}^{-1}$.

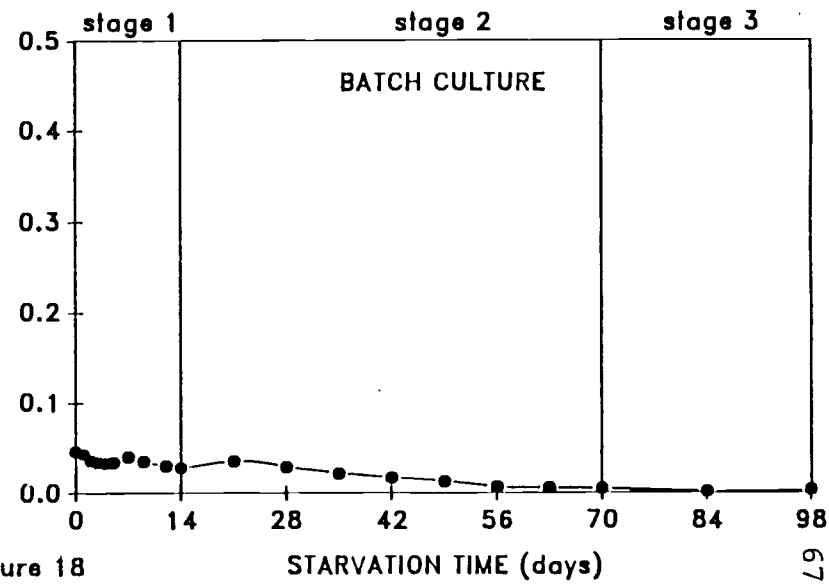
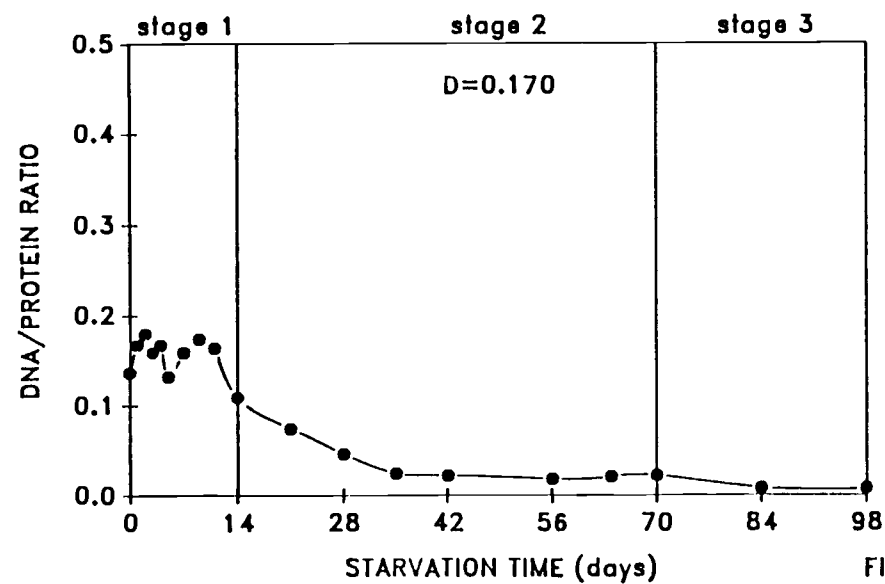
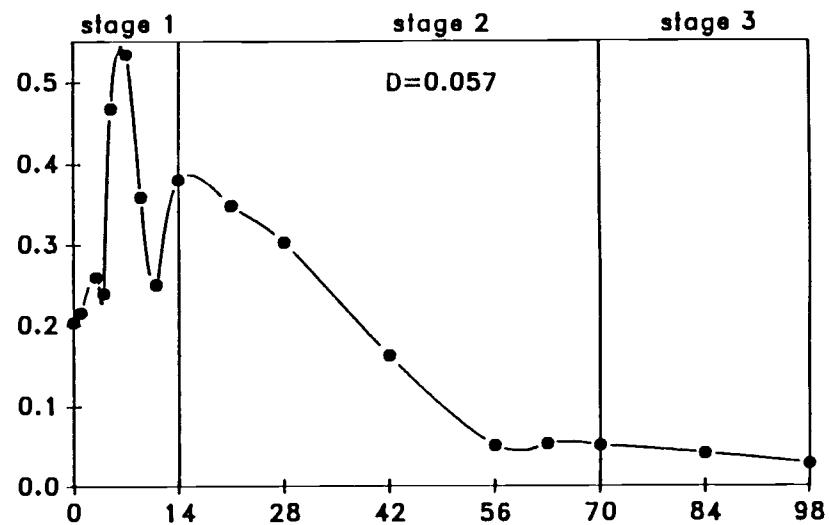
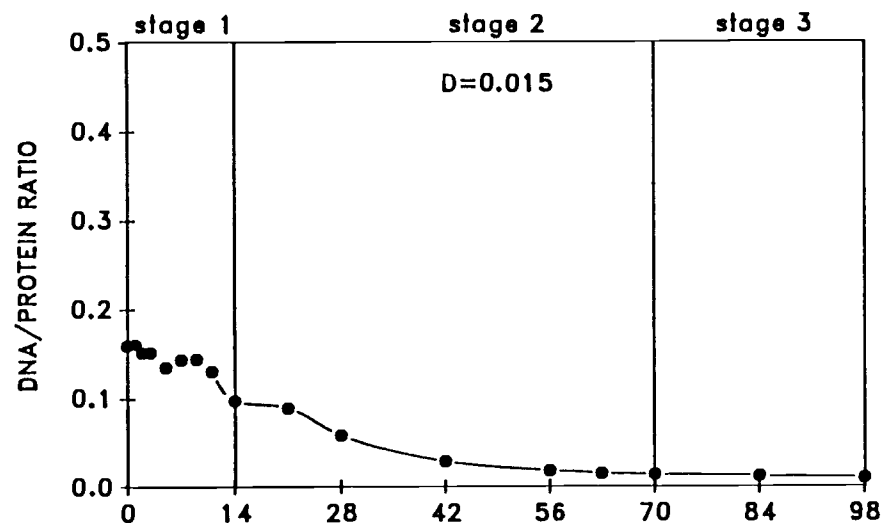


Figure 18

Fig. 19 RNA/DNA ratios with starvation time. Calculated for the following cell populations: Batch culture, $D = 0.170 \text{ h}^{-1}$, $D = 0.057 \text{ h}^{-1}$, and $D = 0.015 \text{ h}^{-1}$.

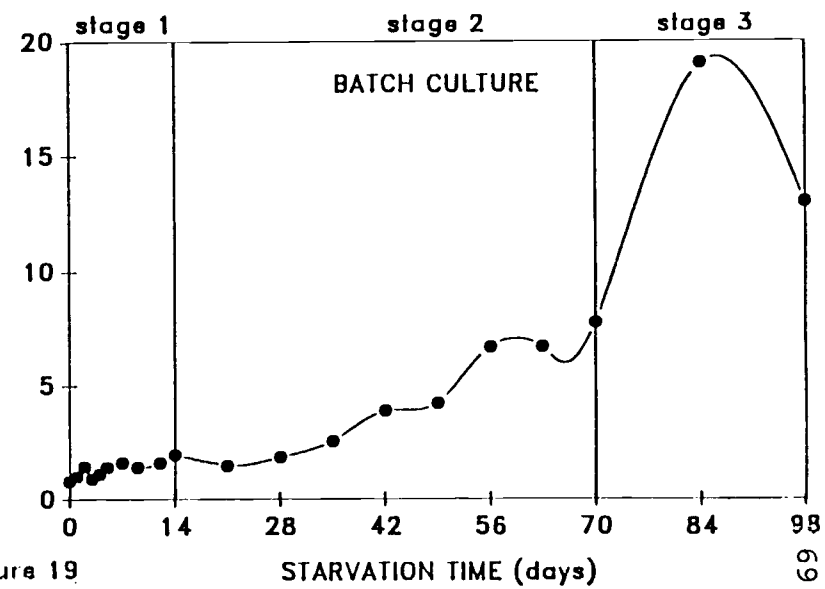
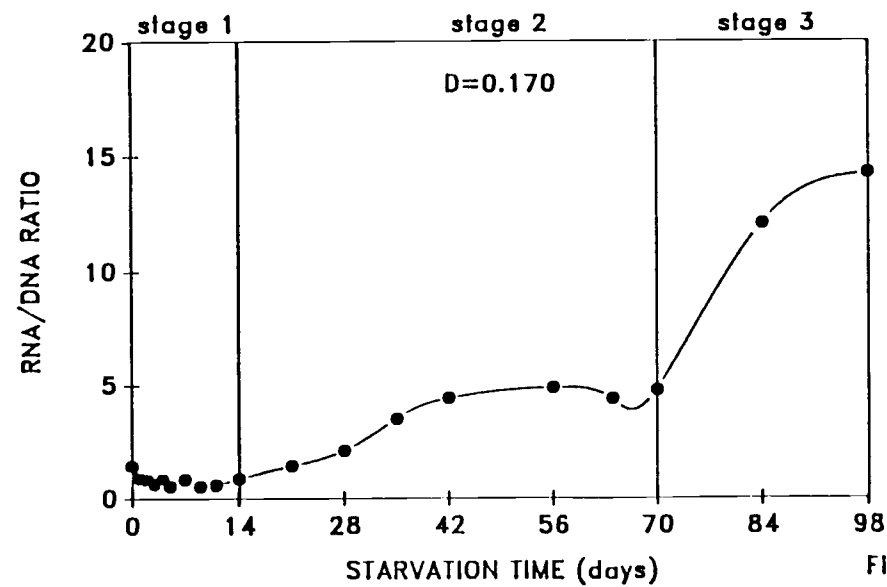
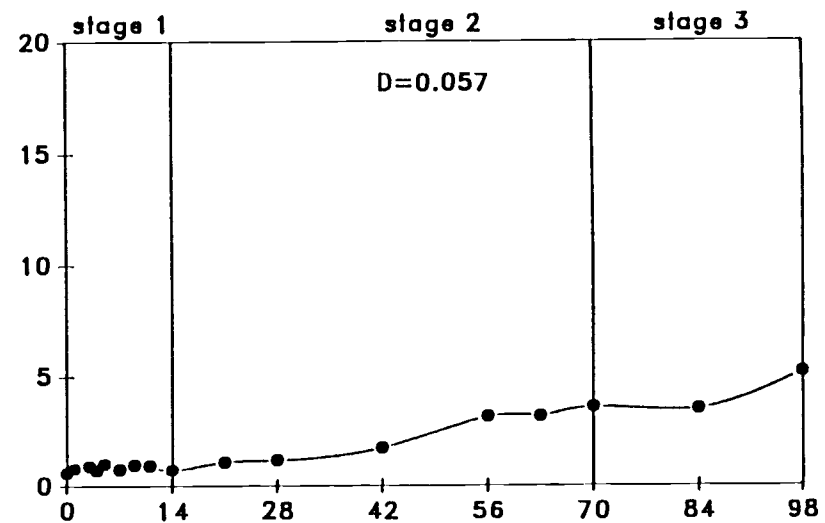
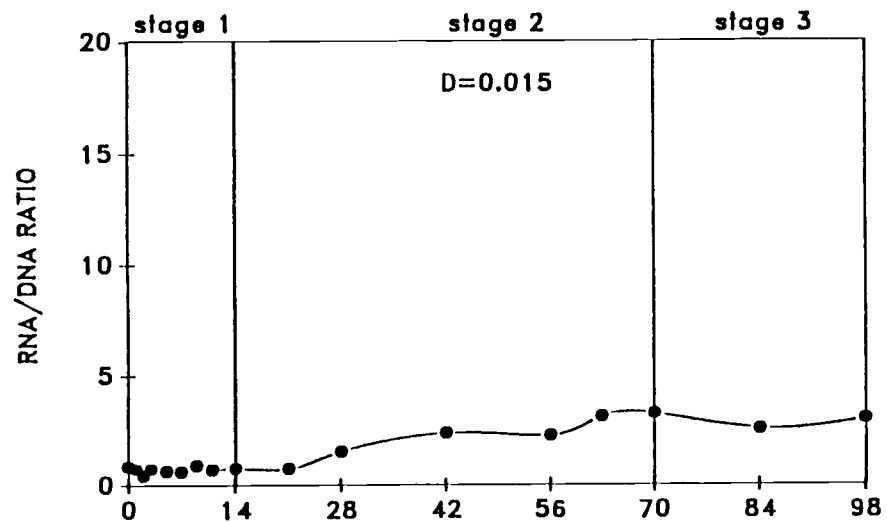


Figure 19

Fig. 20 RNA/protein ratios with starvation time.
Calculated for the following cell populations:
Batch culture, $D = 0.170 \text{ h}^{-1}$, $D = 0.057 \text{ h}^{-1}$, and
 $D = 0.015 \text{ h}^{-1}$.

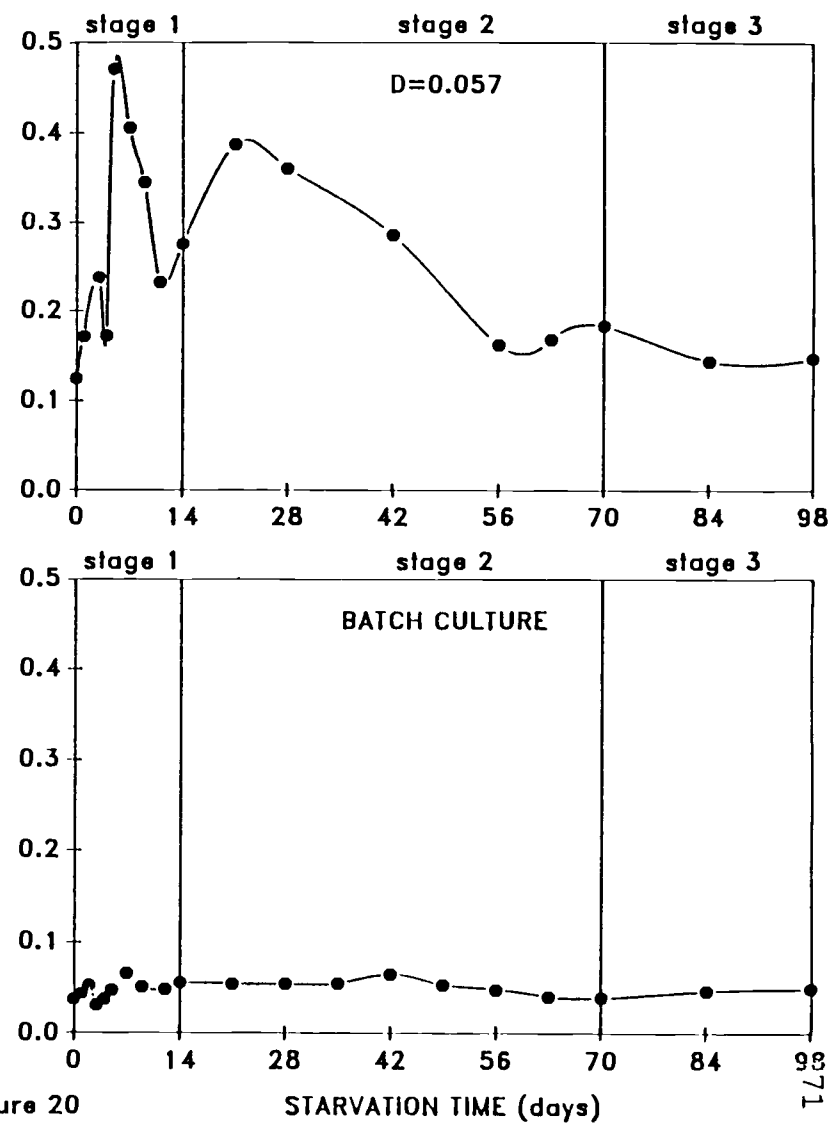
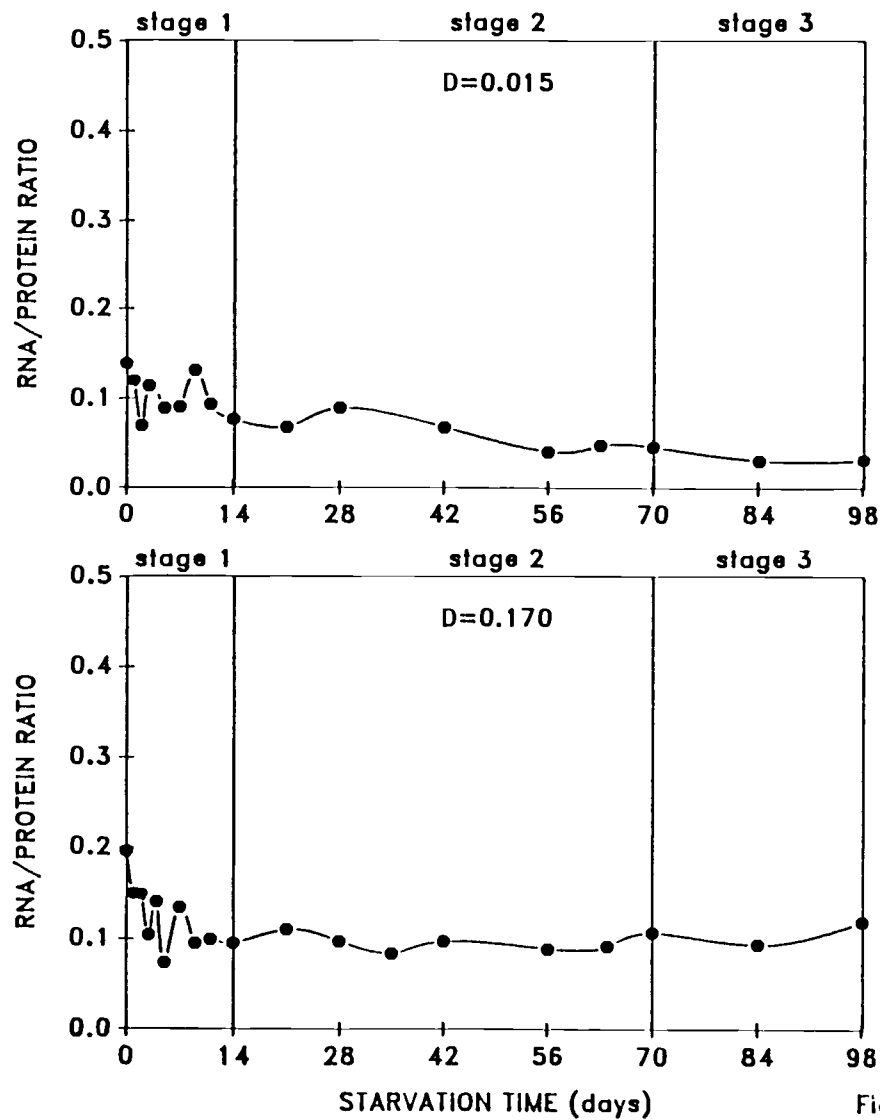


Figure 20

Fig. 21 Protein/DNA ratios with starvation time.
Calculated for the following cell populations:
Batch culture, $D = 0.170 \text{ h}^{-1}$, $D = 0.057 \text{ h}^{-1}$, and
 $D = 0.015 \text{ h}^{-1}$.

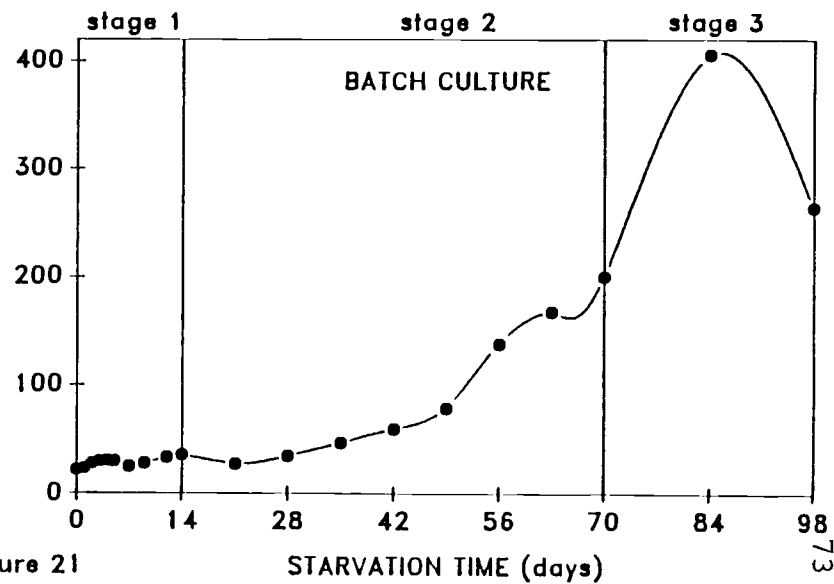
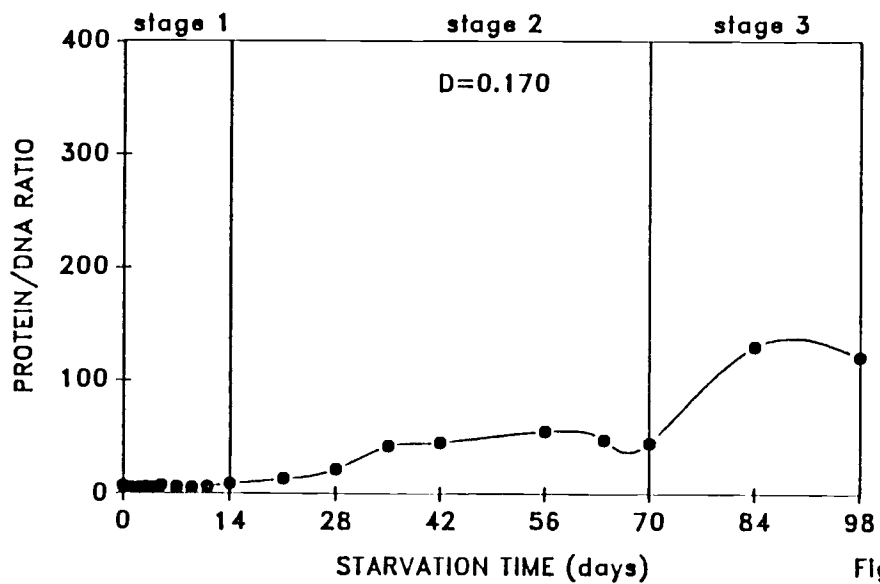
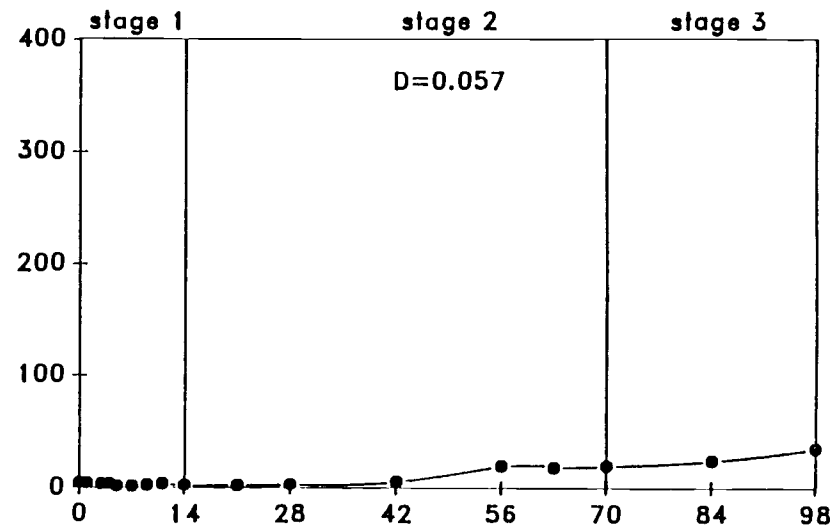
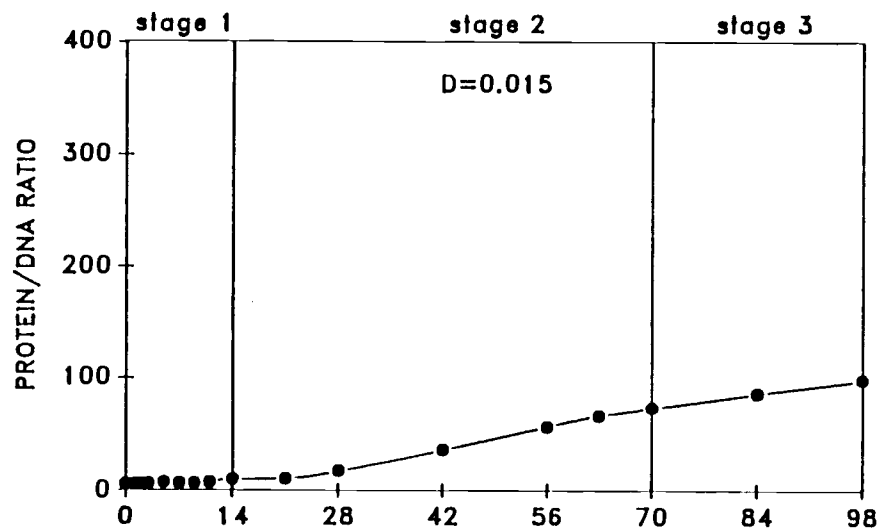


Figure 21

Fig. 22 Protein/RNA ratios with starvation time.
Calculated for the following cell populations:
Batch culture, $D = 0.170 \text{ h}^{-1}$, $D = 0.057 \text{ h}^{-1}$, and
 $D = 0.015 \text{ h}^{-1}$.

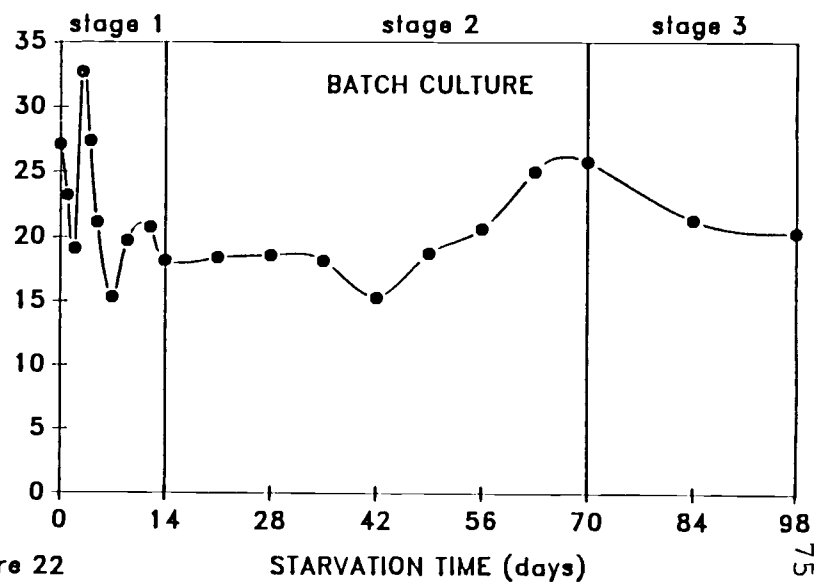
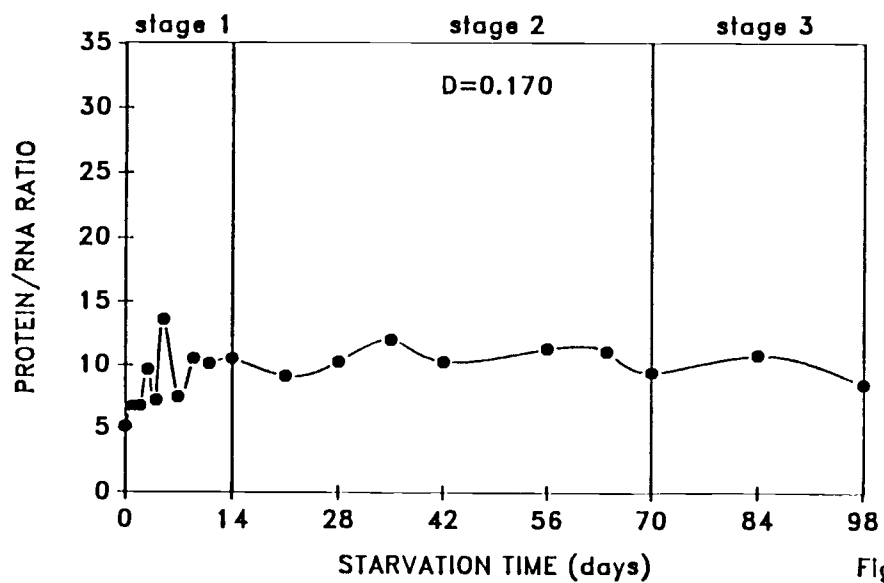
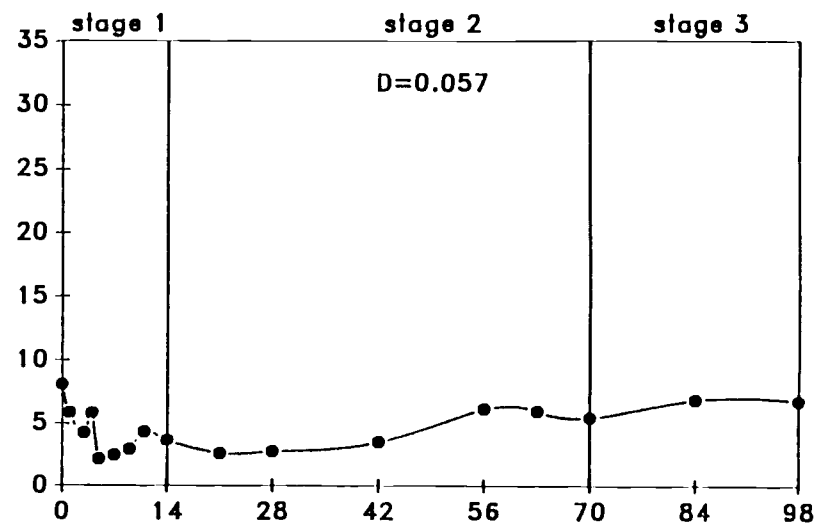
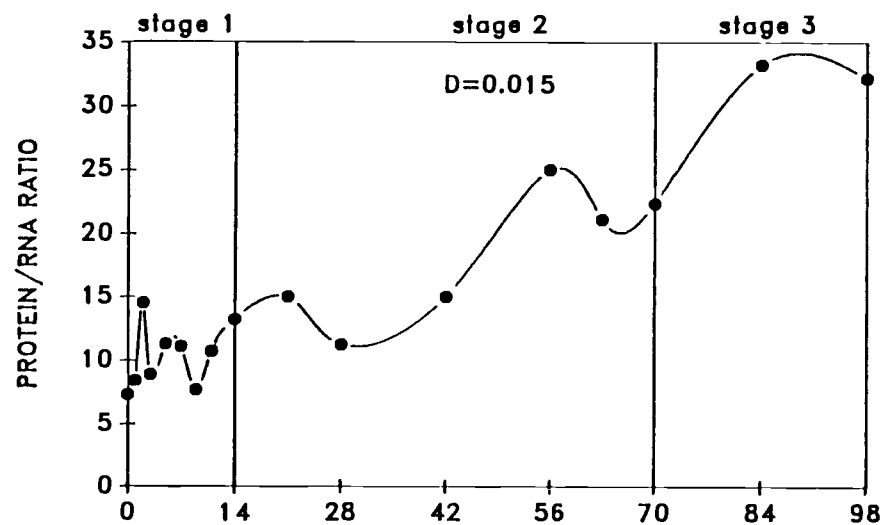


Figure 22

(Fig. 17) for all of cell populations regardless of the original growth rate, even though RNA levels dropped as well. With the exception of the $D = 0.057 \text{ h}^{-1}$ cell population, where the DNA/protein ratios (Fig. 18) during stage 1 and 2 were unusually high, the DNA/protein ratios for the other cell populations were similar. This was due to the rapid loss of protein with respect to DNA in the cells from $D = 0.057 \text{ h}^{-1}$.

The ratios of RNA/DNA (Fig. 19) displayed large amounts RNA with respect to DNA during the later stages. This was especially evident in $D = 0.170 \text{ h}^{-1}$ and batch culture cells. The RNA/protein ratios in $D = 0.057 \text{ h}^{-1}$ cells exhibit large concentrations of RNA relative to protein (Fig. 20) as well as large concentrations of DNA relative to protein (Fig. 18). This could be related to an inability of this cell population to maintain high protein levels, and not due to high losses in DNA or RNA relative to the other cell populations studied.

The increases in protein/DNA ratios (Fig. 21) were primarily due to the losses of DNA observed in the cell populations in general, rather than additional protein production. Again, $D = 0.057 \text{ h}^{-1}$ cells were unable to maintain their protein when compared to the other cell populations. The increases in protein/DNA were most evident in the batch culture cell population which showed the largest increase especially during stage 3. It is also

of interest that the cell populations from $D = 0.015 \text{ h}^{-1}$ and $D = 0.170 \text{ h}^{-1}$ were similar with respect to protein/DNA ratios during the starvation-survival period. This was probably due to the similarity of patterns between the high efficiency state of $D = 0.015 \text{ h}^{-1}$ cells and the high residual state of $D = 0.170 \text{ h}^{-1}$ cells. Protein/RNA ratios (Fig. 22) demonstrated a key factor in that cells from the $D = 0.015 \text{ h}^{-1}$ population were exceptional in maintaining their proteins with respect to the amount of RNA, especially during stage 3. These cells had a higher protein/RNA ratio than even the batch culture cells.

The data pertaining to macromolecule ratios (Fig. 17-22) point out two interesting phenomena. First, both the cell populations $D = 0.015 \text{ h}^{-1}$ and $D = 0.170 \text{ h}^{-1}$ had similar protein/DNA ratios. However, their protein/RNA ratios were much different. The protein/RNA ratio curve for the $D = 0.015 \text{ h}^{-1}$ cells was the only one to demonstrate an increase throughout the entire starvation-survival period. This indicates that the $D = 0.015 \text{ h}^{-1}$ cells did not have the same overall elevated level of protein. The cells from $D = 0.015 \text{ h}^{-1}$ also had a lower residual of RNA, but were still able to maintain and produce protein during the starvation period (Fig. 8). This was possibly due to RNA with high efficiency with respect to energy utilization. Selection for lower energy requirements in RNA appeared to take place primarily when this population

was grown under the slow growth conditions of

$D = 0.015 \text{ h}^{-1}$; equivalent to a $t_d = 46.2 \text{ h}$ (Table 1).

The second phenomena of interest is that cells from the $D = 0.057 \text{ h}^{-1}$ cell population were unable to maintain the relatively high protein residual that occurred in each of the other cell populations. Evidence for this was best shown by the exceptionally high values in the DNA/protein and RNA/protein curves (Fig. 18 and 20). This demonstrates that the $D = 0.057 \text{ h}^{-1}$ cell population was unable to retain the same levels of protein relative to DNA and RNA when compared to the other cell populations. These cells seemed unable to produce or maintain the same starvation proteins as the $D = 0.015 \text{ h}^{-1}$ cells, and they apparently did not have the residual proteins of the $D = 0.170 \text{ h}^{-1}$ or batch culture cell populations. These data also indicate that cells from the faster grown cell populations of $D = 0.170 \text{ h}^{-1}$ and batch culture overproduce RNA and protein, which had accumulated within the cells prior to starvation. This was demonstrated by the high levels of RNA and protein measured throughout the starvation-survival period (Fig. 10 and 11). These cell populations were probably unable to process these high levels of residual macromolecules because of the large drop in endogenous metabolism which occurs early in starvation-survival. The cells from $D = 0.057 \text{ h}^{-1}$ might represent a transitory state between high efficiency of the cells from $D = 0.015 \text{ h}^{-1}$,

and high residuals of RNA and protein in the $D = 0.170 \text{ h}^{-1}$ and batch culture cells.

Summary

It has been demonstrated that a marine bacterium which undergoes extended nutrient deprivation exhibits three stages of starvation-survival. It has also been shown that cells grown under "normal" laboratory conditions are not representative of the bacteria grown at approximate in situ growth rates. This is due to metabolic arrest making residual macromolecules like protein and RNA unavailable and most likely a burden. The slow growth rate ($D = 0.015 \text{ h}^{-1}$) cell population was found to have greater viability and a capability to produce and maintain relatively high levels of starvation proteins. It is hypothesized that this occurs via highly energy efficient ribosomes which are selected for during slow growth. This population of ANT-300 cells was found to achieve and maintain higher surface to volume ratios due to decreased biovolume, which is also a selective advantage for cell survival due to the greater surface to volume ratio maintained throughout starvation-survival. It is concluded that the ANT-300 slow growth rate ($D = 0.015 \text{ h}^{-1}$) cell population most closely represents cells which would be found in situ. Therefore, in order to accurately study the effects of starvation-survival, cells must be grown as

close to in situ growth rates. This should negate the effects of the overproduction of the macromolecules RNA and protein as well as select for a more "natural" physiological and metabolic state.

LITERATURE CITED

1. **Amy, P.S.** 1982. Starvation-survival studies on a marine Vibrio sp. and other selected marine bacteria. Ph.D. thesis. Oregon State University, Corvallis.
2. **Amy, P.S., C. Pauling, and R.Y. Morita.** 1983. Starvation-survival processes of a marine vibrio. Appl. Environ. Microbiol. **45**:1041-1048.
3. **Barber, R.T.** 1968. Dissolved organic carbon from deep waters resists microbial oxidation. Nature **220**:274-275.
4. **Baross, J.A., F.J. Hanus, and R.Y. Morita.** 1974. The effects of hydrostatic pressure on uracil uptake, ribonucleic acid synthesis, and growth of three obligately psychrophilic marine vibrios, Vibrio alginolyticus and Escherichia coli, p. 180-202. In R.R. Colwell and R.Y. Morita (ed.), Effect of the ocean environment on microbial activities. University Park Press, Baltimore.
5. **Broecker, W.** 1963. Radioisotopes and large-scale organic mixing, p. 88-108. In M.N. Hill (ed.), The Sea, Vol. 2. Interscience, New York.
6. **Craig, H.** 1971. The deep metabolism: oxygen consumption in abyssal ocean water. Journal of Geophysical Research **72**:5078-5086.
7. **Carlucci, A.F., and P.M. Williams.** 1978. Simulated in situ growth rates of pelagic marine bacteria. Naturwissenschaften **65**:541-542.
8. **Douglas, D.J., J.A. Novitsky, and R.O. Fournier.** 1987. Microautoradiography-based enumeration of bacteria with estimates of thymidine-specific growth and production rates. Mar. Ecol. Prog. Ser. **36**:91-99.
9. **Francisco, D.E., R.A. Mah, and A.C. Rabin.** 1973. Acridine orange-epifluorescence technique for counting bacteria in natural waters. Trans. Amer. Micros. Soc. **92**:416-421.
10. **Fuhrman, J.A.** 1981. Influence of method on the apparent size distribution of bacterioplankton cells: Epifluorescence microscopy compared to scanning electron microscopy. Mar. Ecol. Prog. Ser. **5**:103-106.

11. **Gaugain, B., J. Barbet, N. Capelle, B.P. Roques, and J.-B. Le Pecq.** 1978a. DNA Bifunctional intercalators. 2. Fluorescence properties and DNA binding interaction of an Ethidium Homodimer and an Acridine Ethidium Heterodimer. *Biochemistry* 17:5078-5088.
12. **Gaugain, B., J. Barbet, R. Oberlin, B.P. Roques, and J.-B. Le Pecq.** 1978b. DNA bifunctional intercalators. 1. Synthesis and conformational properties of an Ethidium Homodimer and of an Acridine Ethidium Heterodimer. *Biochemistry* 17:5071-5078.
13. **Geesey, G.G., and R.Y. Morita.** 1979. Capture of arginine at low concentrations by a marine psychrophilic bacterium. *Appl. Environ. Microbiol.* 38:1092-1097.
14. **Geller, A.** 1986. Comparison of mechanisms enhancing biodegradability of refractory lake water constituents. *Limnol. Oceanogr.* 31:755-764.
15. **Guckert, J.B., M.A. Hood, and D.C. White.** 1986. Phospholipid ester-linked fatty acid profile changes during nutrient deprivation of Vibrio cholerae: Increases in cis/trans ratio and proportions of cyclopropyl fatty acids. *Appl. Environ. Microbiol.* 52:794-801.
16. **Gordon, D.C.** 1970. Some studies on the distribution and composition of particulate organic matter in the North Atlantic Ocean. *Deep Sea Res.* 18:233-243.
17. **Groat, R.G., and A. Matin.** 1986. Synthesis of unique proteins at the onset of carbon starvation in Escherichia coli. *J. Ind. Microbiol.* 1:69-73.
18. **Hobbie, J.E., R.J. Daley, and S. Jasper.** 1977. Use of Nuclepore filters for counting bacteria by fluorescence microscopy. *Appl. Environ. Microbiol.* 33:1225-1228.
19. **Hoff, K.A.** 1984. Bakterier og gyting. Cand.scient.thesis. University of Bergen, Bergen, Norway.
20. **Hood, M.A., J.B. Guckert, D.C. White, and F. Deck.** 1986. Effect of nutrient deprivation on lipid, carbohydrate, DNA, RNA, and protein levels in Vibrio cholerae. *Appl. Environ. Microbiol.* 52:788-793.

21. **Jaan, Å.J., B. Dahllöf, and S. Kjelleberg.** 1986. Changes in protein composition of three bacterial isolates from marine waters during short periods of energy and nutrient deprivation. *Appl. Environ. Microbiol.* **52**:1419-1421.
22. **Jannasch, H.W.** 1967. Growth of marine bacteria at limiting concentrations of organic carbon in seawater. *Limnol. Oceanogr.* **12**:264-271.
23. **Jannasch, H.W.** 1969. Estimations of bacterial growth rates in natural waters. *J. Bacteriol.* **99**:156-160.
24. **Jannasch, H.W.** 1970. Threshold concentrations of carbon sources limiting bacterial growth in sea water, p. 321-328. In D.W. Hood (ed.), *Organic matter in natural waters*. Institute of Marine Sciences Publications, College, Alaska.
25. **Kjelleberg, S., B.A. Humphrey, and K.C. Marshall.** 1982. Effect of interfaces on small, starved marine bacteria. *Appl. Environ. Microbiol.* **43**:1166-1172.
26. **Koch, A.L.** 1971. The adaptive responses of Escherichia coli to a feast and famine existence. *Adv. Microb. Physiol.* **6**:147-217.
27. **Koch, A.L.** 1979. Microbial growth in low concentrations of nutrients, p. 261-279. In E. Shilo (ed.), *Strategies of Microbial Life in Extreme Environments*. Dahlem Konferenzen, Verlag Chemie, Weinheim.
28. **Koch, A.L.** 1980. The inefficiency of ribosomes functioning in Escherichia coli growing at moderate rates. *J. Gen. Microbiol.* **116**:165-171.
29. **Koch, A.L.** 1985. The Macroeconomics of Bacterial Growth, p. 1-42. In M. Fletcher and G.D. Floodgate (ed.), *Bacteria in their natural environments*. Academic Press, London.
30. **Kurath, G., and R.Y. Morita.** 1983. Starvation-survival physiological studies of a marine Pseudomonas sp. *Appl. Environ. Microbiol.* **45**:1206-1211.
31. **Le Pecq, J.-B., M. Le Brett, J. Barbet, and B.P. Roques.** 1975. DNA polyintercalating drugs: DNA binding of diacridine derivatives. *Proc. Nat. Acad. Sci.* **72**:2915-2919.

32. **Malmcrona-Friberg, K., A. Tunlid, P. Marden, S. Kjelleberg, and G. Odham.** 1986. Chemical changes in cell envelope and poly- β -hydroxybutyrate during short term starvation of a marine bacterial isolate. *Arch. Microbiol.* **144**:340-345.
33. **Maniatis, T., E.F. Fritsch, and J. Sambrook.** 1982. *Molecular cloning: a laboratory manual.* Cold Spring Harbor Laboratory, Cold Spring Harbor, N.Y.
34. **Marden, P., M. Hermansson, and S. Kjelleberg.** 1988. Incorporation of tritiated thymidine by marine bacterial isolates when undergoing a starvation survival response. *Arch. Microbiol.* **149**:427-432.
35. **Marden, P., A. Tunlid, K. Malmcrona-Friberg, G. Odham, and S. Kjelleberg.** 1985. Physiological and morphological changes during short term starvation of bacterial isolates. *Arch. Microbiol.* **142**:326-332.
36. **Markovits, J., B.P. Roques, and J.-B. Le Pecq.** 1979. Ethidium dimer: A new reagent for the fluorimetric determination of nucleic acids. *Anal. Biochem.* **94**:259-264.
37. **Menzel, D.W.** 1974. Primary productivity, dissolved and particulate organic matter, and the sites of oxidation of organic matter, p. 659-678. In E.D. Goldberg (ed.), *The Sea*, Vol. 5. Wiley-Interscience, New York.
38. **Menzel, D.W., and J.H. Ryther.** 1970. Distribution and cycling of organic matter in the oceans, p. 31-54. In D.W. Hood (ed.), *Organic Matter in Natural Waters.* Institute of Marine Sciences Publications, College, Alaska.
39. **Morita, R.Y.** 1980. Microbial life in the deep sea. *Can. J. Microbiol.* **26**:1375-1385.
40. **Morita, R.Y.** 1982. Starvation-survival of heterotrophs in the marine environment. *Adv. Microbial. Ecol.* **6**:117-198.
41. **Morita, R.Y.** 1985. Starvation and miniaturization of heterotrophs, with special emphasis on maintenance of the starved viable state, p. 111-130. In M. Fletcher and G. Floodgate (ed.), *Bacteria in the natural environments: the effect of nutrient conditions.* Academic Press, London.

42. **Morita, R.Y.** 1988. Bioavailability of energy and its relationship to growth and starvation-survival in nature. *Can. J. Microbiol.* **45**:In press.
43. **Novitsky, J.A.** 1977. Effects of long term nutrient starvation on a marine psychrophilic vibrio. Ph.D. thesis. Oregon State University, Corvallis.
44. **Novitsky, J.A., and R.Y. Morita.** 1976. Morphological characterization of small cells resulting from nutrient starvation of a psychrophilic marine vibrio. *Appl. Environ. Microbiol.* **32**:617-622.
45. **Novitsky, J.A., and R.Y. Morita.** 1977. Survival of a psychrophilic marine vibrio under long-term nutrient starvation. *Appl. Environ. Microbiol.* **33**:635-641.
46. **Novitsky, J.A., and R.Y. Morita.** 1978. Possible strategy for the survival of marine bacteria under starvation conditions. *Mar. Biol.* **48**:289-295.
47. **Seki, H., J. Skelding, and T.R. Parsons.** 1968. Observations on the decomposition of a marine sediment. *Limnol. Oceanogr.* **13**:440-447.
48. **Smith, P.K., R.I. Krohn, G.T. Hermanson, A.K. Mallia, F.H. Gartner, M.D. Provenzano, E.K. Fugimoto, N.M. Goeke, B.J. Olson, and D.C. Klenk.** 1985. Measurement of protein using Bicinchoninic acid. *Anal. Biochem.* **150**:76-85.
49. **Torrella, F., and R.Y. Morita.** 1982. Starvation induced morphological changes, motility, and chemotaxis patterns in a psychrophilic marine vibrio. *Deuxieme Colloque de Microbiologie marine. Publ. de Centre National pour l'Exploitation des Oceans* **13**:45-60.
50. **Tranvik, L.J., and M.G. Höfle.** 1987. Bacterial growth in mixed cultures on dissolved organic carbon from humic and clear waters. *Appl. Environ. Microbiol.* **53**:482-488.
51. **Watson, S., J. Novitsky, H. Quinby, and F. Valois.** 1977. Determination of bacterial number and biomass in the marine environment. *Appl. Environ. Microbiol.* **33**:940-946.
52. **Williams, P.M., and E.R.M. Druffel.** 1987. Radiocarbon in dissolved organic matter in the central North Pacific Ocean. *Nature.* **330**:246-248.